Appendix A: Inner Heliospheric Sentinels Analyses and Key Tradeoff Studies

1. X-Band HGA Technologies

Detailed mechanical models were developed for several types of antennas to determine the optimum choice based on size, mass, DC power, and ease of implementation. The antennas studied included a paraboloidal solid dish antenna, a parabolic cylinder wire reflector, an electronically scanned flat array, and a mechanically scanned flat array. All antennas were sized to provide the peak gain of a 0.8-m-diameter parabolic dish minus pointing and passive losses. The assumed pointing loss was due to a 0.75° pointing error. All antennas, including associated radomes, had to be compatible with the intense thermal environment of the mission to be considered in the study.

Table A-1 summarizes the findings of the study. An HGA utilizing a paraboloidal solid dish antenna was the heaviest implementation. The mass of this configuration is driven by the mass of the radome and the radome support structure. The radome provides thermal protection and a constant solar pressure as a function of antenna pointing. A similar, although smaller, radome is required for the two flat array antennas.

The parabolic wire cylinder HGA, similar to that flown on Helios, is linearly polarized and therefore has twice the aperture size of the other antennas. This antenna has the highest pointing loss because of the large aperture size, and overcoming this higher pointing loss, in turn, requires increased antenna aperture. Although the parabolic wire cylinder does not require a radome and therefore has the lowest mass by a slight margin, the mass saving is more than offset by the increase in spacecraft structure mass required to accommodate the larger antenna. The parabolic wire cylinder antenna also poses the greatest development risk, as there are no existing X-band antennas of this design.

The two phased array antennas incorporate slotted waveguides similar to those used on the MESSENGER phased array antenna. The electrically steered array uses electronic phase shifters for pointing the beam over the limited range of elevation angles required to maintain Earth contact. The phase shifters, however, must be located down on the despun platform surface for thermal reasons, resulting in 12 transmission paths between the phase shifters and antenna. Each path includes a rotary joint required for gimbaling the antenna into position at the start of the mission.

The mechanically steered phased array requires no phase shifters and is therefore electrically less complicated than the electrically steered antenna. Only two RF transmission paths between the despun platform and the antenna are required (one for each redundant TWTA signal). The mechani-

Table A-1. Summary of technology trade studies for the Inner Heliospheric Sentinels high-gain antenna (HGA).

Antenna Technology	Mass (kg)	Antenna Construction	Bus Power (W)	Net Gain after Pointing Loss and Antenna-Specific Passive Loss (dBic)	Area (m^2)
Paraboloidal dish	34.9	Reflector material is graphite epoxy composite	0.2[a]	33.5	0.5 (0.8-m dia)
Parabolic cylinder (wires)	17.9	Wire material is a platinum-rhodium alloy, wire diameter is 0.2 mm, wire spacing is 2 mm	0.2[a]	33.7	1.56[b] (1.2 × 1.3 m)
Electronically scanned phased array	19.1	Antenna consists of WR90 thin-wall waveguide mounted on an aluminum plate	0.5[c]	33.4	0.36 (0. 6 × 0.6 m)
Mechanically scanned phased array	20.1	Same as electronically scanned phased array	0.2[a]	33.7	0.3 (0.55 × 0.55 m)

Notes:

(a) Bus power for elevation angle gimbal electronics.

(b) Size may decrease if future DSN capability includes linear polarization reception to avoid a 3 dB linear-to-circular polarization mismatch loss.

(c) Bus power for electronic phase shifters.

cally steered array can be designed with passive redundant TWTA inputs. Because of its simpler architecture, low size and mass, and the availability of flight-qualified X-band slotted waveguide array technology, this antenna architecture was chosen as the baseline.

2. X-Band Versus Ka-Band Science Downlink

A detailed study was performed to examine the potential benefit of operating the science downlink at Ka-band (32 GHz) instead of X-band. The potential benefit can be viewed either as a smaller HGA for a given science return or as a higher science return for a given antenna size. A parabolic reflector model was used for this trade study. The Ka-band advantage is measurable in decibels. **Figure A-1** shows the benefit of Ka-band relative to X-band as a function of HGA size and pointing error. For the 1-m-diameter class of HGA being considered for the Inner Heliospheric Sentinels (IHS), the pointing error must be less than 0.3° to enable a significant benefit from Ka-band operation.

A preliminary HGA pointing budget for the IHS spacecraft indicates a worst-case error of 0.8°, which drove our science downlink design to X-band. This pointing error could be improved substantially by placing a star camera on the despun platform; however, the temperature range of the platform currently exceeds that of a star camera, and the field of view from that location may be inadequate. Secondary benefits of an X-band science downlink design include a single-frequency HGA, compatibility with existing space weather ground stations, and overall lower cost relative to Ka-band.

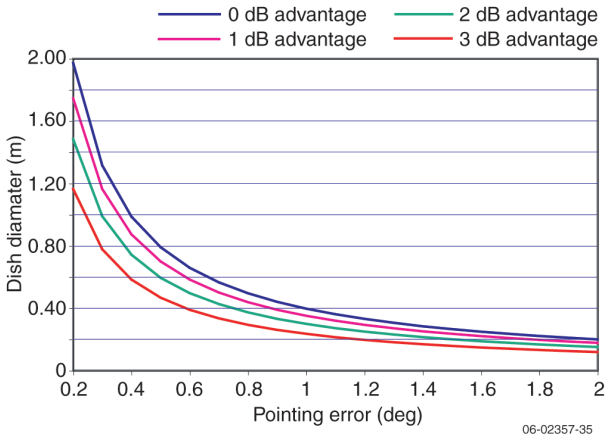

Figure A-1. Ka-band advantage over X-band as a function of pointing error and HGA size.

3. HGA Size Versus DSN Contact Time

The HGA size requirement can be traded off as a function of DSN contact time for a given science return capability. This tradeoff is basically one of spacecraft mass (and associated cost) versus Phase E mission operations cost. A deep space aperture costing formula, available on the DSN website effective April l8, 2005, was used for this analysis. **Table A-2** shows the DSN cost as a function of contact frequency assuming that the four IHS spacecraft are tracked separately and independently. The corresponding HGA antenna size was determined through a combination of RF link analysis and detailed science return analysis.

Based on interactions with the DSN Advanced Planning Office, usage of the 34-m antennas at a loading of one to two contacts per spacecraft per week is reasonable for the Sentinels mission. From that information and the information in **Table A-2,** the size of the IHS antenna can be narrowed down to a range of 0.7 to 1 m in diameter. A parabolic reflector model was used for this trade study. To minimize DSN cost and loading, we have adopted a contact frequency of once per week per spacecraft, resulting in the need for an HGA having performance equivalent to that of a 1-m diameter dish (about 36 dB of gain at X-band).

4. ELV Separation Strategy

Spacecraft deployment from the launch vehicle will involve seven separate deployments, one for each of the four spacecraft and three inter-spacecraft structures. Different scenarios were evaluated in making this final decision, as there was a desire to minimize the number of deployments, or at the very least minimize the number of immediate deployments so as to reduce the possibility of contact between the various pieces.

One option involved leaving the inter-spacecraft structure attached to the bottom of each spacecraft. This would reduce the number of deployments to four. Due to thermal considerations, however, the structure would eventually need to be separated from the spacecraft. Thus the question became one of early operations with the structure attached. In this configuration the aft low-gain antenna (LGA),

Table A-2. Deep Space Network usage cost versus high-gain antenna size.

DSN Contacts per Spacecraft each Week	Total DSN Contacts each Week	Yearly Cost ($M)	Parabolic HGA Diameter (m)
0.25	1	0.5	2
0.5	2	1.1	1.4
1	4	2.6	1
2	8	6.7	0.7

Notes:

DSN Assumptions:
- Fiscal year 2005 costs
- Each pass includes 8 hours of science downlink plus 1 hour of pre/post pass calibration.
- 34-m DSN antennas
- Spacecraft are tracked separately and independently
  - Not co-located within beamwidth of the DSN antenna
  - Not tracked sequentially during a pass

RF Link Assumptions
- X-band operation
- 75 W_{RF} (150 W_{DC}) TWTA
- HGA overall efficiency = 55%
- 5 kbps continuous science plus 30% margin returned from each spacecraft.

located on the bottom of the spacecraft, would almost certainly require a deployed boom, adding the undesirable complication of a boom deployment. Moreover, the structure would block the star scanner, and the spacecraft–structure combination may not be a major-axis spinner. Additional analysis and design would be required to resolve the stability question.

A possible resolution to these issues would be to make the inter-spacecraft structure a truss design, potentially alleviating the need for a boom deployment. However, without going into a detailed analysis of this type of design, it was unknown if the LGA could provide enough gain through the structure. It was also questionable as to whether the star scanner field of view would still be partially obstructed, and whether a truss-structure could meet the launch vehicle modal frequency requirements for a stacked configuration.

Leaving the structure attached to the top of a spacecraft was another option considered. This would alleviate issues with the aft LGA and star scanner, but there could still be issues with spin stability (not a major-axis spinner). The structure would eventually still need to be deployed, since the HGA on the top of the spacecraft would be blocked by the structure.

The decision to have seven deployments was felt to be technically viable and to reduce complications with spacecraft design and operations. Collision avoidance is mitigated by requiring the launch vehicle to alter the direction in which the various pieces are ejected. Additionally, the launch vehicle already has the power switching resources to control the individual separations, thus alleviating the need for these services to be added to the spacecraft.

5. Spacecraft Post-Separation Distances

The four IHS spacecraft and three inter-spacecraft structures are stacked on a single launch vehicle. The separation sequence consists of seven separations, one each for the four spacecraft and three inter-spacecraft structures. The nominal release scenario starts at approximately L + 2 hours and ends 2 hours later, with spacecraft released every 40 minutes and the three adapter rings released in between. In this nominal scenario, the release of all of the spacecraft should occur within view of a DSN station. The spacecraft release (ΔV) directions would nominally be 5° to 10° apart to increase any possible close approach distances to an acceptable level (close to the separation distance at release). This release scenario has been discussed with Kennedy Space Center personnel and appears feasible with an Atlas V or Delta IV launch vehicle.

Spacecraft release and separation analysis was performed for the release scenario just described. Four spacecraft with masses assumed to be 750 kg each were released from a stacked configuration. An Atlas V second-stage mass of 2200 kg was assumed for this analysis. In addition, the analysis assumed that the spring release mechanism nominally provided a ΔV of 1.0 m/s to a single spacecraft in the direction of ecliptic normal (relative to the pre-release state). It was also assumed that the spring applied an equal total impulse in the opposite

direction during the release. If the spacecraft release ΔV error could be reduced to less than about 5% to 6% for this scenario, there should be no post-release close approaches of the spacecraft even if the spacecraft were all released in the same direction. Larger release ΔV errors can result in post-release close approaches if the spacecraft release ΔΩs are applied in the same direction. However, if the spacecraft release ΔV directions are offset by 5° to 10°, post-release close approach distances can be increased significantly to a level not much smaller than the release distance, and this is the release scenario that would nominally be used. **Figure A-2** shows the IHS-to-IHS range with spacecraft release ΔVs of 1.0 m/s normal to the ecliptic plane; the ranges for other combinations of spacecraft as a function of time are larger. **Figure A-3** shows the effect of a 5° offset in release ΔV direction on the post-separation close approach distance resulting from a difference in the spacecraft release ΔV magnitudes relative to the pre-release state (–10% and +10% errors, respectively). **Figures A-2 and A-3** were generated using the September 4, 2015, launch case trajectory data. This analysis did not include the release of the three connecting rings in addition to the four spacecraft, but the release scenario proposed above should be effective for that scenario as well.

6. Spacecraft Flip Maneuver

The science team has expressed the possible desire to perform a flip of the spacecraft, in which the spin-axis direction is flipped 180°. This type of maneuver could be possible with the IHS spacecraft, but the tank capacity would have to be slightly increased to ensure there was sufficient propellant to do so. A technique that will minimize the propellant required to do the flip has been identified.

First, this maneuver will require a significant amount of time, potentially days. As the spacecraft spin-axis precesses, the 20-m wire booms will not immediately follow. It will take some time for them to "catch up." If the maneuver is performed too quickly the wire booms could become entangled. As a result, the flip would have to be divided into small segments where the spacecraft precesses, and then time is allotted for the wire booms to stabilize.

Second, the flip maneuver requires a substantial amount of propellant. Precessing a spacecraft spinning at 20 rpm would require many thruster firings. One way to reduce the number of firings, and thus the amount of propellant required, is to lower the spin rate. **Table A-3** shows the current best estimate of the propellant required to perform the flip at various spin rates and two spacecraft masses, the nominal mass and the mass with 30% margin. The propellant shown in the table includes the propellant mass needed to spin down, flip the spacecraft, and

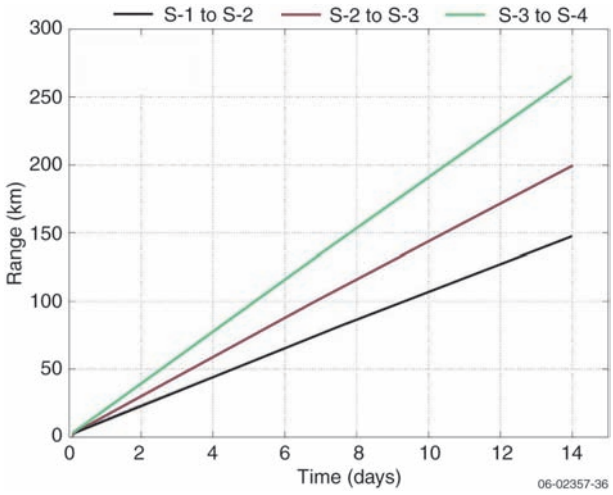

Figure A-2. Inner Heliospheric Sentinels spacecraft post-release separation distance. S-1 through S-4 denote the first though fourth spacecraft released. Release ΔV = 1 m/s normal to ecliptic plane for all IHS spacecraft; separation range is over 2 weeks. Time is referenced to launch.

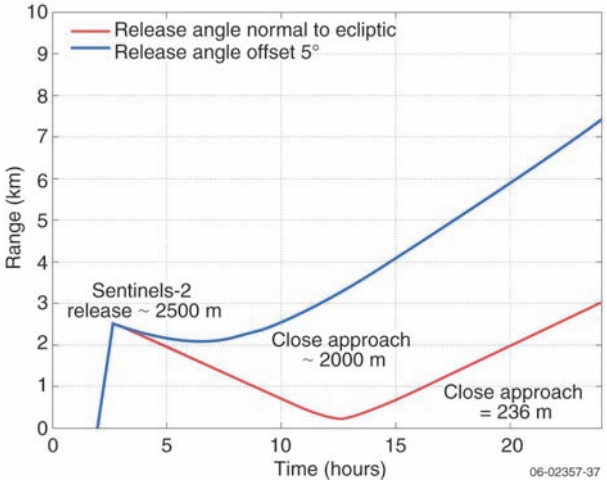

Figure A-3. Inner Heliospheric Sentinels spacecraft post-release separation distance showing range between Sentinels-1 and Sentinels-2 with 5° offset in release ΔV direction. Release ΔV = 0.9 m/s and 1.1 m/s for Sentinels-1 and Sentinels-2, respectively.

Table A-3. Current best estimate of propellant required to flip the IHS spacecraft based on minimum spin rate during maneuver and spacecraft mass.

Minimum spin rate during maneuver (rpm)	Propellant required with nominal spacecraft mass (kg)	Propellant required including 30% mass margin (kg)
3	3.3	4.2
5	4.1	5.3
10	6.0	7.8
20	10.0	12.9

spin back up to 20 rpm. Propellant usage is a function of the number of thruster pulses and the on-time for each pulse. The number of pulses required for the flip varies with the square of the spin rate, while the on-time is inversely proportional to spin rate.

There are restrictions on when the flip maneuver can be performed. The spin rate cannot be reduced when the spacecraft is close to the Sun due to thermal issues. It also cannot be reduced when the solar array output is close to the load power.

The proposed IHS propulsion subsystem allows an extra 2.0 kg of propellant (total) to be loaded into the tanks. As **Table A-3** shows, the current design would not accommodate a flip maneuver.

7. Minimum Perihelion Distance

An optimization study was performed to characterize the Sentinels mission trade space in terms of key parameters in an optimal relationship to one another. The result of this study reveals the sensitivity of spacecraft mass to perihelion distance. An Excel-based model was built to determine optimal structure and solar array form factors in order to minimize structure mass.

The model determines optimum spacecraft and solar array form factors in order to minimize overall spacecraft mass. Key variables are spacecraft body diameter and height and solar array length. Driving parameters include:

- Perihelion distance
- Thermal characteristic for specific form factor at perihelion distance
- Expendable launch vehicle (ELV) C_3 capability
- Four spacecraft on single ELV
- ELV fairing constraints
- Spacecraft power load
- Inertia ratio to ensure major axis spinner

The minimum perihelion distance is the largest driver of spacecraft mass. At a perihelion of 0.23 AU and with the spacecraft power load expected for the IHS mission, solar cell technology is on the edge of feasibility. As the perihelion distance is reduced, a larger fraction of solar array area must be allocated to Optical Surface Reflectors (OSRs) to maintain acceptable panel temperatures. As a result, the solar array area must increase in order to supply the same amount of power. For example, the solar array area doubles from 0.25 to 0.20 AU due to this relationship. **Figure A-4** illustrates the relationship between spacecraft mass and perihelion distance. Based upon this optimization study, the perihelion distance for the IHS mission was selected to be 0.25 AU so that four-spacecraft mission (from a mass standpoint) could launch on an affordable ELV. A reduced perihelion becomes feasible if an ELV with a greater lift capability is used. Reduced perihelion has additional effects not considered in the model used to relate spacecraft mass to perihelion distance. The thermal environment for components exposed to the Sun becomes more severe. This applies to instrument apertures, antennas, thrusters, and Sun sensors. Solar pressure increases, but this is not likely to be a concern.

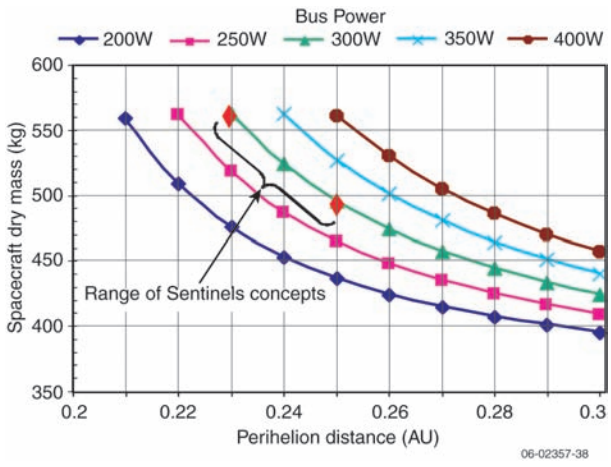

Figure A-4. Inner Heliospheric Sentinels spacecraft mass sensitivity to perihelion.

8. Radial versus Stacked Configuration

Two spacecraft configuration concepts were studied: stacked and radial. The selected stacked configuration stacks the spacecraft on top of one another, with a jettisoned inter-spacecraft structure between spacecraft. The radial configuration has the four spacecraft sitting side by side on top of a common launch vehicle dispenser. The dispenser includes four spin-up tables to spin up the spacecraft prior to deployment. The radial spacecraft configuration is narrower and taller than the stacked version. **Figure A-5** illustrates the radial configuration before and after deployment. **Figure A-6** illustrates the dispenser configuration. **Table A-4** compares the system parameters for the radial and stacked configurations.

The areas where the stacked configuration is superior make the stacked configuration inherently simpler and lower in risk than the radial configuration. The areas where the radial solution are superior are less important (e.g., differences in structure thickness between spacecraft), or they indicate minor concerns with the stacked configuration that can be managed (180° rotation of HGA and potential for contact between spacecraft at separation). The stacked configuration was selected because it carries the lower risk and is the simpler solution.

9. Selection of Heliocentric Spacecraft Orbits

Various final heliocentric spacecraft orbit configurations were analyzed. Originally, low C_3 Venus trajectories using a single Venus flyby were analyzed; final heliocentric orbits of 0.50 to 0.95 × 0.72 AU were achieved. The Sentinels science team felt it would be desirable to have perihelion of at least one of the spacecraft in the 0.20- to 0.30-AU range. Using higher C_3 Venus trajectories (maximum of ~30 km^2/s^2) with higher hyperbolic excess velocities (~10 km/s or more) at the Venus flybys and using three Venus flybys, perihelions as low as ~0.23 AU were achieved. After more detailed thermal analysis the minimum perihelion was constrained to 0.25 AU. Initially, the spacecraft performed between one and three Venus flybys and achieved final orbits between ~0.25 × 0.72 and 0.51 × 0.93 AU. The Sentinels science team felt it would be desirable to have perihelion of all of the spacecraft at approximately 0.25 AU and to achieve more significant heliocentric separation of the spacecraft early in the mission; this resulted in the current baseline

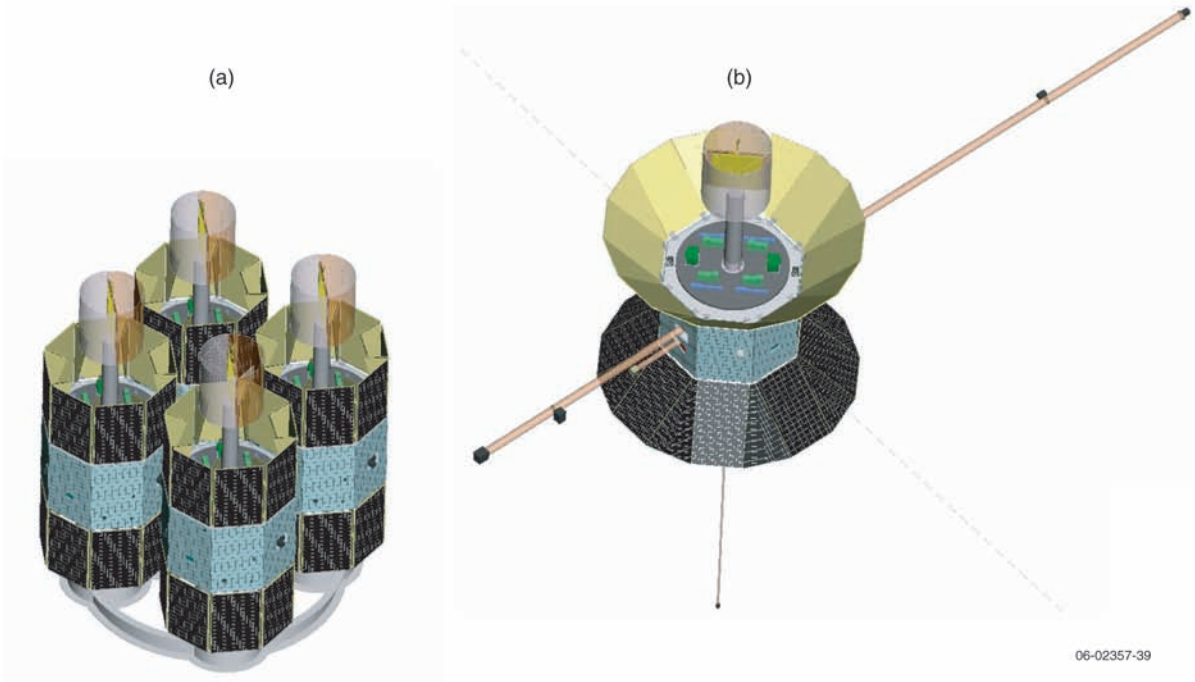

Figure A-5. Radial configuration of the Inner Heliospheric Sentinels spacecraft in (a) launch configuration and (b) deployed configuration.

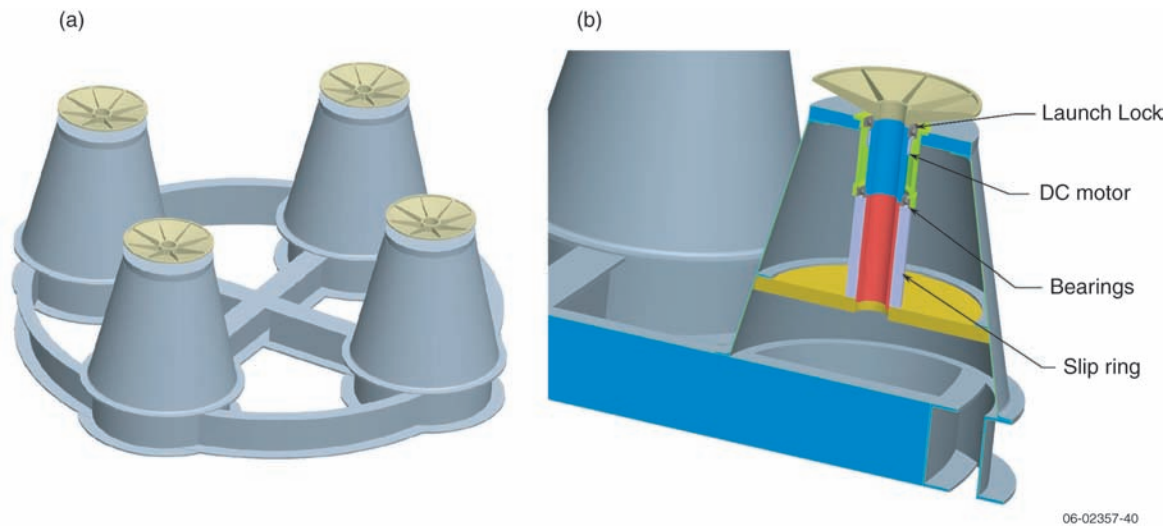

Figure A-6. (a) Dispenser for radial configuration; (b) radial dispenser spin-up mechanism.

Table A-4. Comparison between stacked and radial spacecraft configurations.

System Parameter	Stacked Configuration	Radial Configuration	Winner
Solar array	Fixed	Deployed with complicated baffle	Stacked
Thermal design	Large area for radiator on bottom deck	Small area for radiator on bottom deck	Stacked
Major axis spinner	Yes, at separation	Only after booms deployed, requires active nutation control	Stacked
Launch vehicle (LV) adapter complexity	Simple rings to interface stack to LV and between spacecraft	Complicated, one large adapter that incorporates four spin tables	Stacked
Separation Sequence	Requires seven serial deployments; uses LV rotation to spin up spacecraft. Design must ensure no contact between spacecraft when separating	Deploy spacecraft in pairs; LV must power up spin tables to spin up spacecraft. Reduced concern for contact between spacecraft during separation.	Radial
HGA configuration	Requires 180° rotation to get HGA into operational configuration	Does not require 180° rotation to get into operational configuration (but gimbal still needed to point HGA)	Radial
Mass	Greater average spacecraft mass (706 kg), but comparable total launch mass (3192 kg)	Lower average spacecraft mass (563 kg), but comparable total launch mass (3100 kg)	Even
Spacecraft similarity	The thickness of each spacecraft's internal support structure is different	All spacecraft have identical internal support structures	Radial

scenario with two of the spacecraft performing three Venus flybys and the other two spacecraft performing four Venus flybys. The science team requested significant heliocentric separation of the 0.25 AU perihelion right ascensions. This was achieved by modifying the Venus flyby scenarios.

10. Eclipses and Earth Occultation During Venus Flybys

Eclipses of excessive duration during Venus flybys could cause the required battery capacity to increase. For Type 1 trajectories (2012 launch), flyby periapsis moves toward the sub-solar point (the point at which the Sun is directly overhead) during the multiple flyby scenario; there should be no Venus eclipse periods for these trajectories. For Type 2 trajectories (2014, 2015, 2017 launches), flyby periapsis moves away from the sub-solar point during the multiple flyby scenario; Venus eclipse periods are possible for these trajectories. For an August 21, 2015, launch case, shadow periods were analyzed for the Sentinels-1 trajectory. There

were umbra periods on flyby 2 (1385-s duration) and on flyby 3 (933-s duration) for the Sentinels-1 spacecraft. Similar maximum shadow durations would be expected for other Type 2 trajectories since they have similar geometry. For the February 8, 2014, launch case, the maximum umbra duration was 1424 s on flyby 2 for the Sentinels-1 spacecraft. The battery (sized for the launch load requirement) can easily accommodate eclipses of these durations. In order to minimize the load on the battery, prior to the eclipse the spacecraft would be placed in a low-power mode by turning the instruments off and selecting the medium-power transmitter.

Earth occultation during Venus flybys is a potential concern, because communications with the Earth would be disrupted. Earth occultation during the Venus flybys was not analyzed in detail; however the maximum duration of Earth occultation events (if there are any) would be similar to that of the shadow events. Since no critical events such as maneuvers would occur during the Venus flybys (see Table 5.3-1), these events would not have a significant effect.

11. High-Gain Antenna Gimbal Angles Based on Orbit Trajectories

The angle between the heliocentric orbit plane and the spacecraft-to-Earth line determines the range of operation for the spacecraft high-gain antenna (HGA) gimbal. This parameter was analyzed for the 2/18/2014, 8/26/2015, 9/4/2015, 3/9/2017, and 3/19/2017 launch trajectory cases. For the spacecraft with the largest heliocentric ecliptic inclinations (2/8/2014, 3/9/2017, and 3/19/2017 launch cases), that angle was approximately 5° to 9° in the days after launch and decreased to less than 1° at the first Venus encounter. Between Venus flybys 2 and 3 of Sentinels-3 and Sentinels-4 (the period of higher ecliptic inclination), that angle was approximately 6.4° maximum. With a heliocentric ecliptic inclination of 1.3° and with maximum heliocentric ecliptic declination near aphelion, the maximum value of that angle after the final flyby would be approximately 5.4°.

The spacecraft can accommodate large positive gimbal angles (HGA pointing upward from the spacecraft body), but the maximum negative gimbal angle that can be accommodated is restricted to –7°. This was not an issue with the trajectories studied, but it could be a concern for other trajectories. Large gimbal angles always occur when the spacecraft–Earth distance is small, which is when maximum downlink rate can be achieved and a large volume of data can be dumped from the solid-state recorder (SSR). If the required gimbal angle exceeds the gimbal capability, SSR playback would be effectively halted during these high-data-rate periods because downlink communications must use the medium-gain antenna (MGA) instead of the HGA. For these trajectories, the determination of whether the IHS constellation is deployed "upside down" (HGA on the ecliptic south side of the spacecraft) or "right side up" could be based on minimizing the duration of large negative gimbal angles in order to enhance science data return.

12. Antenna Assembly Gimbal Design

An antenna assembly consisting of an HGA, an MGA, and one low-gain antenna (LGA) is gimbal-mounted within a radome on the despun platform. During the mission the antenna assembly is gimbaled in elevation by up to +15°/–7° to keep the HGA pointed at Earth. The gimbal does double duty by holding the antenna assembly in a compact position during launch and, after separation and early operations, rotates the antenna assembly approximately 180° into an operational state with a clear field of view past the solar arrays at all necessary gimbal angles. **Figure A-7** illustrates the gimbal design. The gimbal rotation is accomplished by a gear linkage mounted inside the center support tube powered by a drive actuator at the base of the tube. This design provides a benign thermal environment for the actuator. The actuator is a space-qualified motor from CDA InterCorp. A bearing shaft is attached to the drive actuator and is held in place by a set of precision bearings. At the opposite end of the bearing shaft is a gear shaft also held in place with bearings having a spur gear mounted to the tip. The spur gear will drive the antenna assembly about its rotation axis using a bevel gear attached to the RF rotary coupler housing.

13. Determination of Solar Array Tilt Angle

The IHS solar arrays are tilted relative to the spin axis. The optimum tilt angle is primarily driven by its effect on spacecraft radiator effectiveness. Radiator panels placed on the bottom spacecraft deck view the back of the hot solar arrays. As the tilt angle

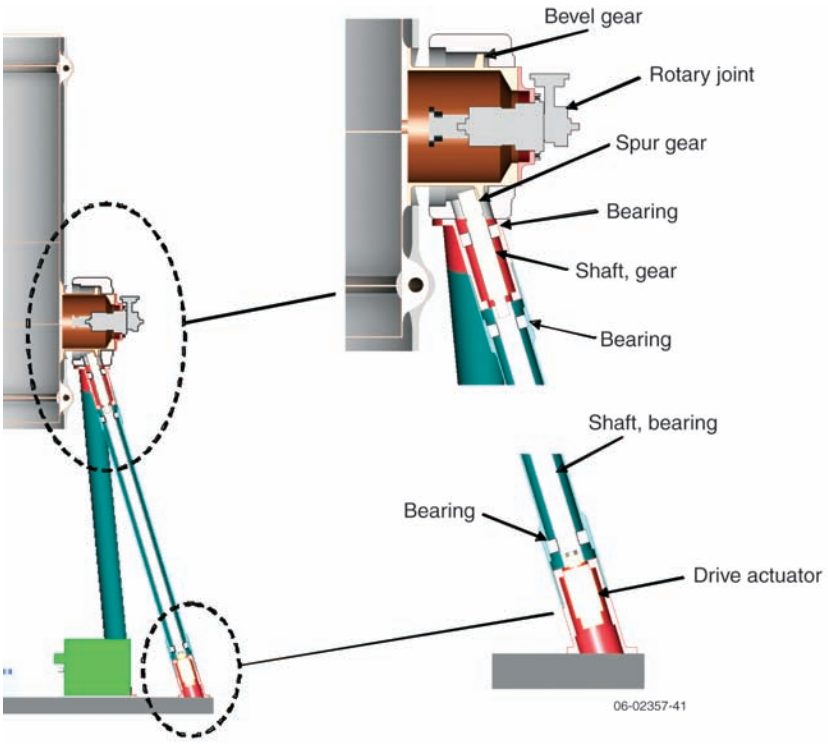

Figure A-7. Antenna assembly gimbal design shown with thermal blankets removed.

increases, the radiators have an improved view of deep space and will run cooler, which enhances removal of heat from the spacecraft bus. However, if the tilt angle is made too large, the power generation effectiveness of the solar arrays drops too much and the solar array would become unacceptably massive. A second factor is that for a given tilt angle, the temperature of the solar array will decrease as the solar cell packing factor is decreased (and the fraction of optical solar reflectors increases). As the solar array runs cooler, the radiator sink temperature also decreases. As a further constraint, the combination of tilt angle and packing factor must limit the solar array temperature to no more than 180°C at perihelion. The process used to determine the optimum tilt angle was to find the minimum angle at which the radiator sink temperature and solar array temperature were acceptable for a reasonable packing factor.

Four solar array tilt geometries were modeled in order to quantify the radiator sink temperature as a function of solar array tilt angle and packing factor. **Figure A-8** illustrates the results of this analysis. Solar array tilt angles less than 45° translate into radiator sink temperatures well above 0°C, which would not permit effective cooling of the spacecraft. A tilt angle of 45° would allow a reasonable packing factor of ~0.5 and an acceptable radiator sink temperature. As shown in **Figure A-9**, the solar array temperature is also acceptable with a tilt angle of 45°. Therefore, the spacecraft was designed with a solar array tilt angle of 45°. It is possible that a tilt angle slightly more or less than this would be better in terms of spacecraft mechanical design, solar array mass, radiator effectiveness, and instrument fields of view, but feasibility has been demonstrated with this angle.

Figures A-8 and **A-9** are based on simple analyses done early in the IHS study. For example the final spacecraft diameter was not used and the effect of the HGA blocking the back of the upper solar arrays (and causing their temperature to increase) was not included. **Figure 5-18** in the report more accurately shows how the packing factor varies with perihelion in order to maintain panel temperature at or below 180°C.

14. Inner Heliospheric Sentinels Initial RF Acquisition Strategy

The post launch initial RF acquisition of four IHS spacecraft will present unique challenges to the

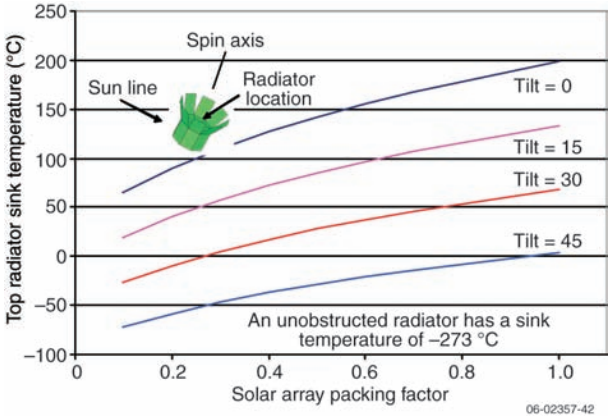

Figure A-8. Radiator sink temperature vs. packing factor and tilt angle.

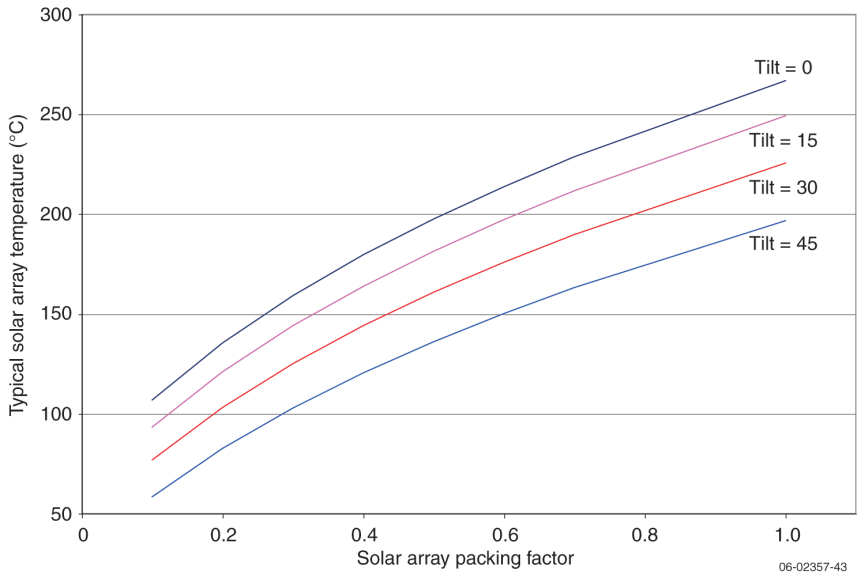

Figure A-9. Solar array temperature vs. packing factor and tilt angle.

Deep Space Network (DSN) and mission operations team. Of principal concern during the launch and initial acquisition process is to monitor the health and safety of each spacecraft. In the unlikely event of a detected anomaly, commanding of the spacecraft maybe necessary or desirable to resolve or troubleshoot the anomaly before proceeding to normal operations. Finally, radiometric tracking is also critical to determine the magnitude of any launch error that may have been imparted by the launch vehicle. Radiometric tracking is used to effectively point the DSN antenna and to determine any critical maneuvers that may be necessary as the result of the launch error.

Of primary of concern to the initial acquisition phase will be the availability of limited ground station resources to support command, telemetry, and radiometric tracking of four spacecraft. The analysis shown below is for a single launch opportunity of September 4, 2015; the entire launch window and launch opportunities were not analyzed. The resources identified herein are currently available in 2006. During the first 24 hours of operation, DSN has insufficient capability to remain in simultaneous contact with all four spacecraft. The initial acquisition strategy outlined use both DSN and Universal Space Network (USN) resources to support telemetry, command, and radiometric tracking of all four IHS spacecraft during initial RF acquisition and early operations.

Figure A-10 shows the relative separation distance of each spacecraft for the September 4, 2015, launch opportunity. The top graph shows the relative separation distance for the first 14 days from launch and the bottom plot shows a more refined view of the first 24 hours from launch. All four spacecraft can be viewed from a single DSN complex over this 2-week period based on the beamwidth of a 34-m antenna, the known Earth distance, and the small separation distance.

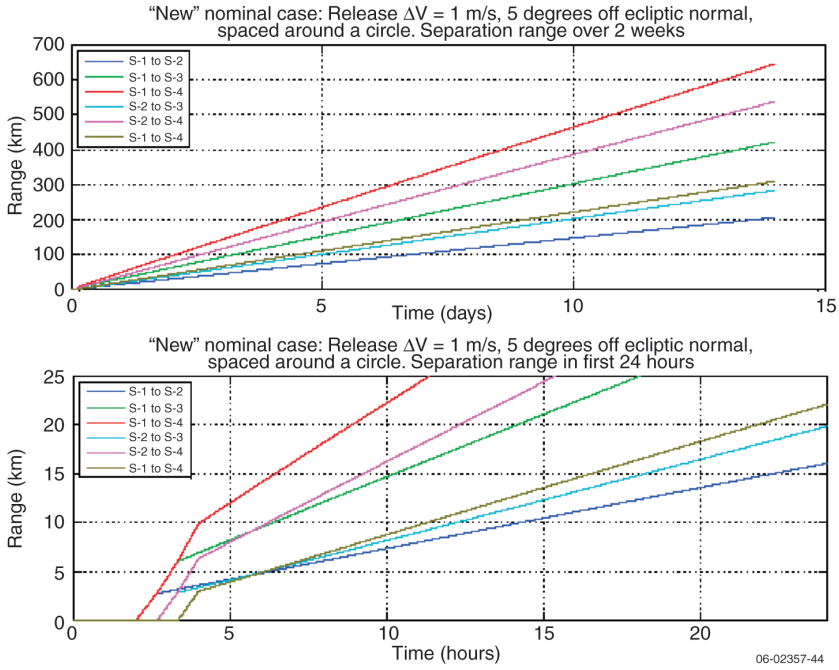

Figure A-10. Relative separation distance (km) of Sentinels-1 through 4 for the first 14 days after launch (top). The bottom plot shows the first 24 hours after launch.

Figure A-11 shows an initial acquisition strategy for first contact. Since the number of DSN-compatible ground station assets available for spacecraft commanding, telemetry reception, and radiometric tracking exceeds the resources available, a "round-robin" approach was developed. The spacecraft separate from the launch vehicle at 40-minute intervals. Two 34-m antennas (DSS-34 and DSS-45) at the DSN Canberra station and antennas at the USN Dunagara and Hartebeesthoek stations will be used for initial contact with the four spacecraft. USN stations have previously supported the early operations for deep space missions such as New Horizons. The USN stations have no X-Band uplink command or radiometric capability and will be used solely for telemetry reception.

Both the DSS-34 and DSS-45 antennas will acquire Sentinels-1 when it separates from the launch vehicle. The USN Dunagara station will provide backup real-time telemetry for Sentinels-1. When Sentinels-2 separates from the launch vehicle, the DSS-45 antenna will transition from Sentinels-1 to Sentinels-2. The USN Hartebeesthoek station will provide backup real-time telemetry for Sentinels-2. DSS-34 and Dunagara will continue to track Sentinels-1. At this point uplink and downlink capability for the first two spacecraft will be established through DSN antennas, and backup telemetry established through USN antennas.

When Sentinels-3 separates from the launch vehicle, the DSS-34 antenna will transition from Sentinels-1 to Sentinels-3, providing uplink and downlink capability for Sentinels-3. Real time telemetry from the USN Dunagara station will continue to supply the health of Sentinels-1 but this station cannot provide a command capability. Radiometric tracking of Sentinels-1 will have been collected for 80 minutes and a solution of the launch errors could now be pursued to aid in DSN and USN antenna pointing.

When Sentinels-4 separates from the launch vehicle, the DSS-45 antenna will be released from Sentinels-2. Real-time telemetry from Sentinels-2 will continue to be received at the USN Hartebeesthoek station to allow monitoring of critical spacecraft health and safety, but as with Sentinels-1, there will no longer be a command capability. At this point, uplink and downlink capability have been established with Sentinels-3 and 4, but downlink capability only with Sentinels-1 and 2. The European Space Agency (ESA) station at New Norica, Western Australia, is an additional asset that could be used for uplink commanding and radiometric tracking of Sentinels-1 or 2 during this period.

The USN stations identified (as well as others at other locations on Earth) can continue to receive spacecraft telemetry out to a spacecraft range of 0.002 AU, which corresponds to 12 hours after launch. These stations, together with DSN stations, can provide simultaneous telemetry coverage of all four spacecraft, and uplink commanding and radiometric coverage of two spacecraft at a time. After

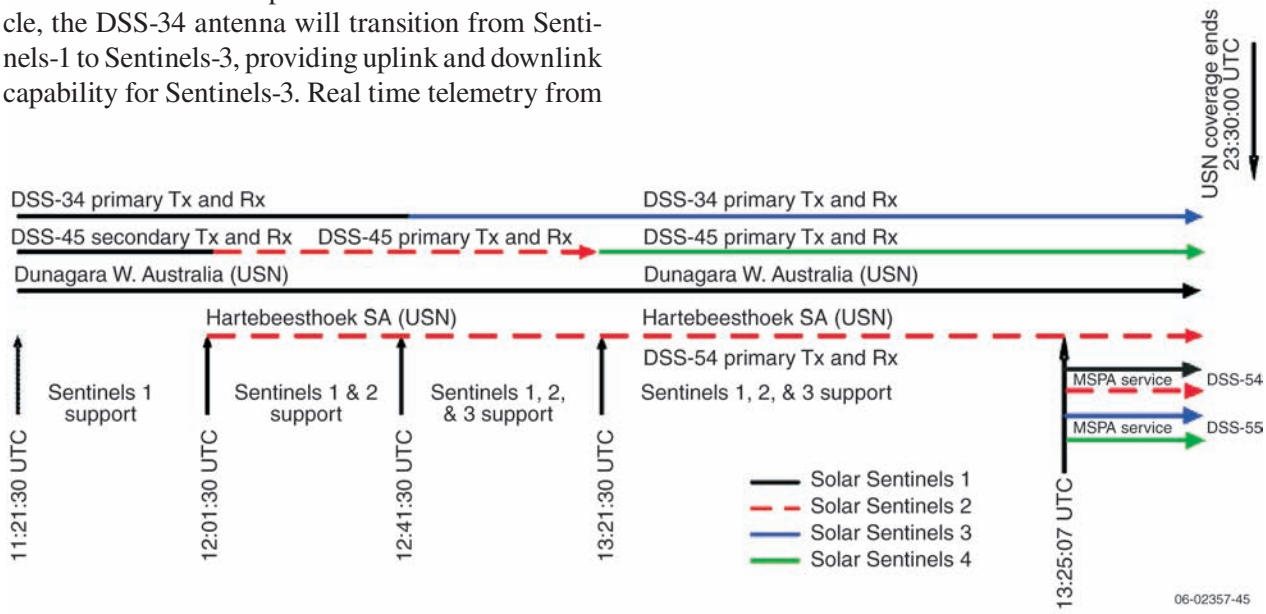

Figure A-11. Initial RF acquisition strategy for the IHS spacecraft using DSN and Universal Space Network (USN) assets.

day L + 12 hours, in order to achieve continuous telemetry coverage of all four spacecraft, the program must utilize the Multiple Spacecraft Per Aperture (MSPA) capability of DSN stations. MSPA allows a single antenna to process two or more downlink signals, but is limited to a single command uplink. After the spacecraft separate beyond the beamwidth of a 34-m antenna, this service will not longer be possible. At this point it will only be possible to remain in contact (uplink and downlink) with two spacecraft at a time by utilizing two 34-m dishes at each DSN station.

15. Bearing and Power Transfer Assembly (BAPTA)

The bearing and power transfer assembly (BAPTA) is an important component of the spacecraft. It allows the top platform to be despun from the rest of the spinning spacecraft so that the HGA and MGA can be pointed toward Earth. The BAPTA also allows the passage of three RF and up to 55 non-RF signals between the spinning spacecraft and the despun platform. The proposed BAPTA design from Boeing as shown in **Figure A-12** has a redundant brushless DC motor and resolver. The control electronics are redundant, but physically separate from the BAPTA. Components having heritage from other flight programs include the resolver, preload spring, slip-ring structure and slip-ring brush/ring interface for the non-RF channels, and bearings. The motor and the RF rotary joint will be slightly modified from their heritage designs. Since all of the parts are either re-used without changes or slightly modified from heritage designs, the BAPTA presents a low risk to the mission. The average lifespan (to date) of all BAPTAs produced by Boeing since 1972 for spinning spacecraft is about 13 years, well in excess of the IHS mission life goal of 5 years. This average lifespan has been limited by the spacecraft lifetime; all of the BAPTAs were operating at the retirement of the spacecraft.

The BAPTA control performance greatly exceeds what is necessary. It is capable of controlling the phase of the despun platform to an accuracy of 10 arcsec. This accuracy could degrade by an order of magnitude and the HGA pointing accuracy requirement of 0.8° would still be met.

Two of the BAPTA RF channels are waveguide based and can easily accommodate the power level of the high-power traveling wave tube antenna (TWTA). The third channel is coax-based and can support the medium-power TWTA continuously. The high-power TWTA can be accommodated on the coax channel for short periods (approximately 5 minutes). This allows ample time for the spacecraft autonomy system to correct the configuration of the RF subsystem if it were to be inadvertently commanded to an invalid state with a high-power TWTA connected to the MGA or LGA on the despun platform.

16. Study of Alternate RF Subsystem Configurations

The baseline design for the Inner Heliospheric Sentinels RF subsystem locates all the RF subsystem electronics (except for the antennas) on the lower deck of the spacecraft. A block diagram of the baseline RF subsystem is shown in **Figure A-13**. This topology requires three RF channels through the bearing and power transfer assembly (BAPTA) for the signals going to the antennas on the despun platform.

The baseline RF subsystem design was chosen after comparing designs containing a single RF channel BAPTA and a dual RF channel BAPTA. The single-channel case has all the subsystem electronics mounted to the despun platform. The dual- and

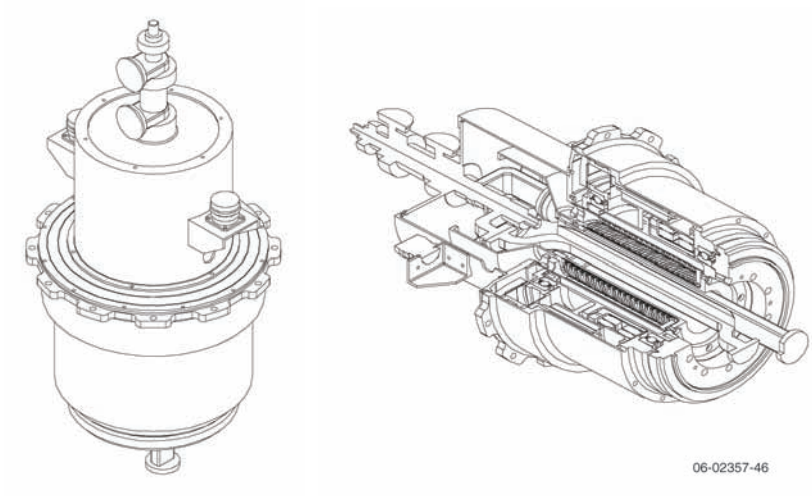

Figure A-12. Proposed BAPTA design from Boeing.

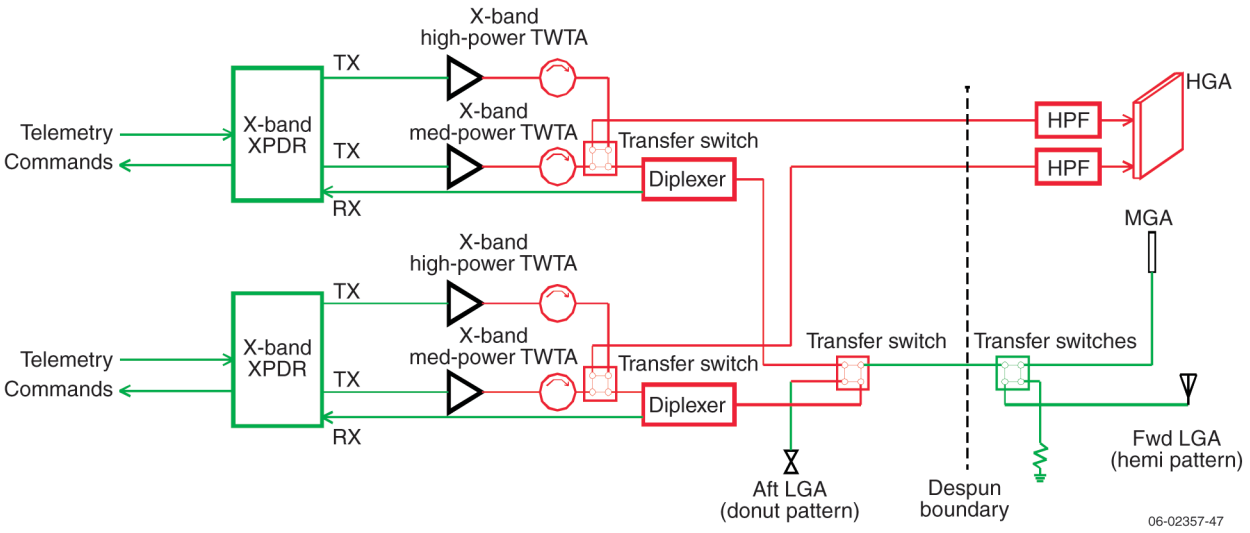

Figure A-13. Baseline IHS telecom system block diagram with three-channel BAPTA.

three-RF channel BAPTA allows the RF subsystem electronics to be moved off the despun platform; this results in significant advantages

Location of RF subsystem electronics: spacecraft body vs. despun platform

Locating RF subsystem electronics on the spacecraft body provides the following benefits:

1. **Simplified despun platform:** The despun platform no longer has to be designed to radiatively couple ~100W of dissipation on the platform to the spacecraft body. The platform no longer has to accommodate a network of heat pipes to spread the heat across the platform. The mass of the platform can be decreased. The platform no longer has to be thermally isolated from the BAPTA .
2. **Increased transmitter power:** The high-power transmitters can be conductively coupled through the spacecraft structure to radiators on the bottom deck rather than radiatively coupled to the spacecraft body from the platform. This allows the transmitter power to be increased and to utilize the excess power available from the solar arrays.
3. **Increased science data rate:** The high-power transmitter power can be increased, allowing more the return of more science data. If the high-power transmitter was located on the platform, it would be thermally limited to 150 W, and the science data rate would be limited to 5000 bps (rather than the baseline 5900 bps).
4. **Reduced number of non-RF signals in the BAPTA:** The number of non-RF signals that the BAPTA must accommodate is reduced from ~100 to ~50. This also allows the elimination of a despun platform multiplexer electronics box that would be required to squeeze all of the required I/O needed for a one-channel BAPTA configuration into only 100 channels.

RF Subsystem with One Channel BAPTA and Dual-Feed HGA

A block diagram of the RF subsystem with a one-channel BAPTA is shown in **Figure A-14**. All of the RF subsystem electronics are located on the despun platform. A despun platform multiplexer (DPM) is required to reduce the number of non-RF signals to ~100. The basic RF subsystem topology is identical to the baseline RF subsystem configuration except that the despun boundary has been moved.

RF Subsystem with Two-Channel BAPTA and Dual-Feed HGA

A block diagram of the RF subsystem with a two-channel BAPTA is shown in **Figure A-15**. All of the telecom equipment except the antennas is on the spacecraft body shown to the left of the despun

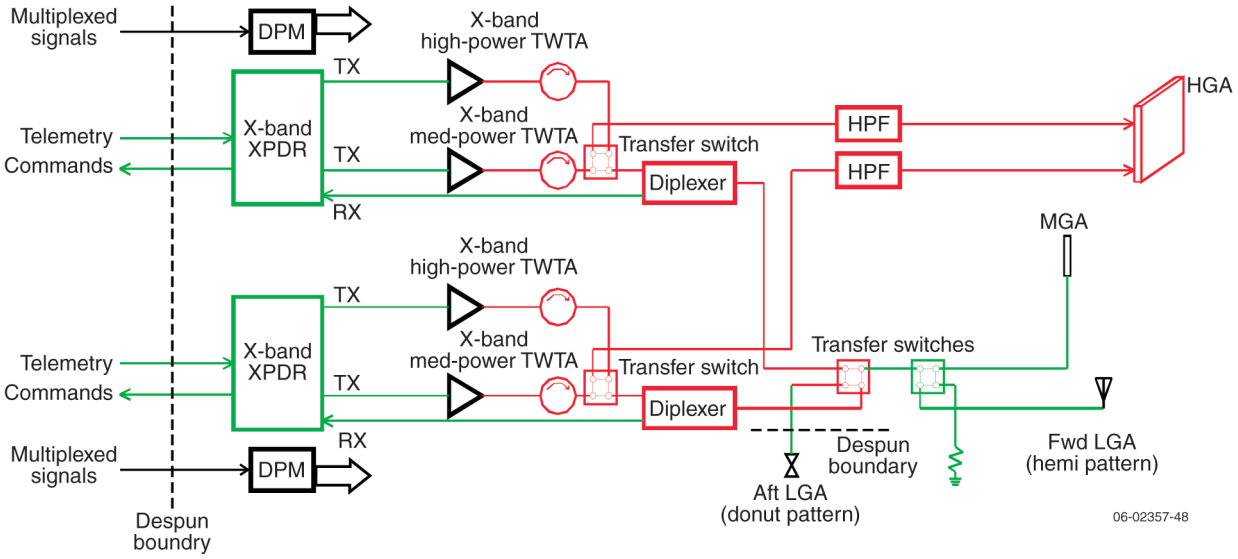

Figure A-14. Block diagram of telecom system with one-channel BAPTA.

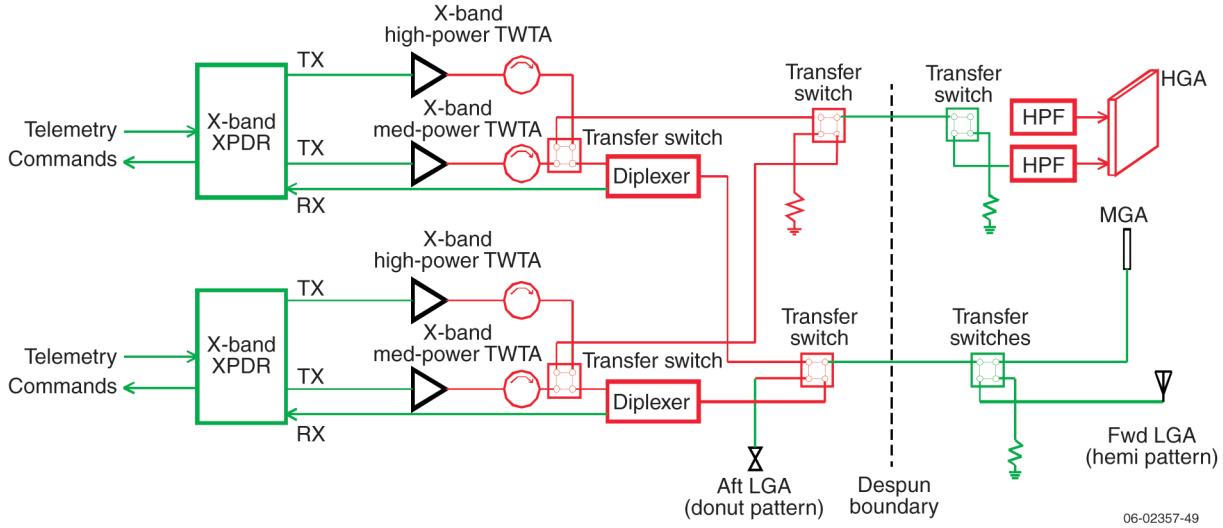

Figure A-15. Block Diagram of Telecom System with Two-Channel BAPTA.

boundary. Two additional transfer switches are needed in the connections to the HGA.

RF Subsystem with Two-Channel BAPTA and Single-Feed HGA

A block diagram of the RF subsystem with a two-channel BAPTA but also with a single-feed high gain antenna is shown in **Figure A-16**. All of the electronics are on the spacecraft body. An additional switch is needed compared to the baseline design, and the HGA only has one input.

Conclusion

The three-channel BAPTA configuration appears to be optimal. The reliability of a two-channel BAPTA is not believed to be significantly better than a three-channel BAPTA. The height of the three-channel BAPTA does not drive the spacecraft height. The reliability of a dual-feed versus a single-feed HGA needs to be evaluated. The pros and cons of the four potential RF subsystem configurations are summarized in **Table A-5**.

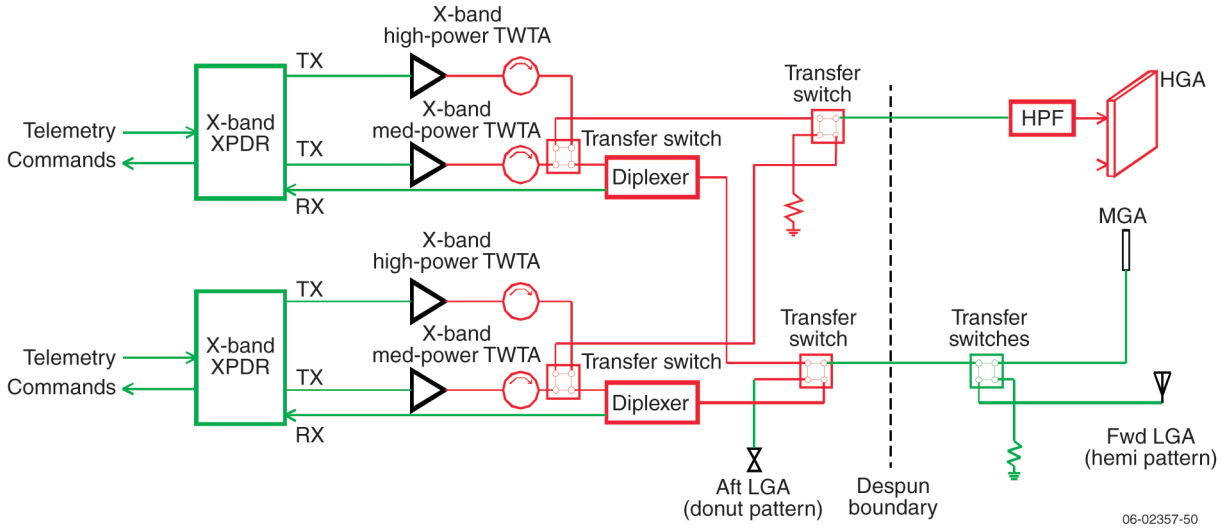

Figure A-16. Block Diagram of Telecom System with Two-Channel BAPTA and Single-Feed High Gain Antenna

Table A-5. RF subsystem configuration tradeoff summary.

RF Subsystem Configuration	Pro	Con
1-channel BAPTA, dual-feed HGA	• Simplest RF rotary joint	• Complex platform design requires heat pipes • Platform power must be dissipated by radiating to spacecraft body • High-power transmitter limited by thermal constraints, reduces science data rate • Platform must be thermally isolated from BAPTA • BAPTA must accommodate ~100 non-RF signals • A redundant despun platform multiplexer is needed to accommodate all of the signals needed by the components on the platform
2-channel BAPTA, dual-feed HGA	• Simplifed thermal design • Transmitter power and science data rate can be increased • BAPTA only has to accommodate ~50 non-RF signals • A despun platform multiplexer is not required	• Two additional switches in HGA feed • Introduction of potential single-point failures
2-channel BAPTA, single-feed HGA	• Simplifed thermal design • Transmitter power and science data rate can be increased • Minimizes number of RF switches • BAPTA only has to accommodate ~50 non-RF signals • A despun platform multiplexer is not required	• One additional switch in HGA feed • Introduction of potential single-point failures
3-channel BAPTA, dual-feed HGA (baseline design)	• Simplifed thermal design • Minimizes number of RF switches • Transmitter power and science data rate can be increased • BAPTA only has to accommodate ~50 non-RF signals • A despun platform multiplexer is not required	• Most complicated RF rotary joint

17. Alternate IHS Spacecraft Mechanical Configurations

The baseline IHS design has fixed (non-deployed) solar arrays and an HGA that is simply rotated to become operational. This design is simple and low risk because there are essentially no spacecraft deployables, although a jettisoned spacer cylinder is required between each spacecraft. Other stacked configurations were studied that would reduce the launch mass by utilizing a folding HGA and folding solar arrays. Two of these configurations are compared to the baseline IHS configuration.

Cartoons of the IHS spacecraft baseline configurations and two alternative configurations are shown in **Figure A-17**. For each, the launch and deployed configurations are shown. The configurations are compared in **Table A-6**.

A fourth configuration was studied that further reduced the stowed size of the solar array by adding a second hinge to each solar array panel. This configuration did not provide any additional overall mass reduction due to the mass of the additional hinges and deployment mechanisms required, and so it was not studied further.

The alternative spacecraft configurations have two advantages:

- Total launch mass is reduced.
- The three inter-spacecraft cylinders and associated separation systems are not needed.

The alternative spacecraft configurations have several disadvantages, however:

- HGA mechanical complexity is greatly increased; the HGA must be folded up and stowed for launch, including a folded and deployed radome.
- Solar array complexity is greatly increased; solar arrays must be folded up and stowed for launch, including additional mechanisms.
- A solar array baffle must be deployed along with the solar array to block sunlight from illuminating the backs of the solar array panels after they are deployed.
- The aft LGA must be on a deployed mast instead of a fixed mast (in the baseline configuration, the aft LGA mast on an upper spacecraft is nestled within the HGA radome of a lower spacecraft).
- Some of the solar array panels will be shaded until the spacecraft is separated from the upper stage and the panels deployed. This may increase the required battery capacity compared with the baseline configuration.
- Some of the thrusters are blocked with the body-fold configuration prior to solar array release.

The baseline configuration was selected even though it requires a slightly more capable launch vehicle because spacecraft complexity and risk are reduced relative to the alternative configurations.

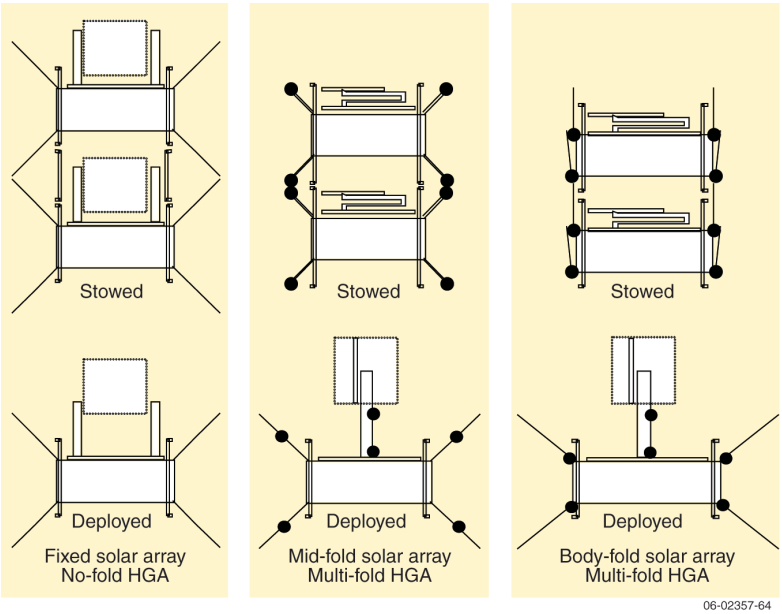

Figure A-17. IHS Baseline and alternate mechanical configurations.

Table A-6. Comparison of IHS mechanical configurations.

Parameter	Spacecraft Configuration		
	Baseline IHS	**Mid-Fold Solar Array**	**Body-Fold Solar Array**
Primary structure material	Isogrid aluminum panels	Aluminum honeycomb panels	Aluminum honeycomb panels
Solar array	Fixed, non-deployed	Deployed, hinge in middle	Deployed, hinge at S/C mount
Solar array baffle	Not needed	Simple (Kapton between solar array panels)	Complex
HGA mechanical complexity	Simple: 180° rotation but no hinges or deployment mechanisms required	Complex: multiple hinges and deployment mechanisms; limited space; deployed radome	Complex: multiple hinges and deployment mechanisms; very limited space; deployed radome
Aft LGA	Nondeployed	Deployed	Deployed
Spacer cylinders & separation systems	Spacers needed, 6 separation systems	No spacers needed, 3 separation systems	No spacers needed, 3 separation systems
Total launch mass	3192 kg	2774 kg	2697 kg
Mass reduction compared with baseline	–	418 kg	495 kg
Solar array power available before separation from stack	Full power from array	Reduced power from array	Reduced power from array
Thruster impact	None	None	Blocked until solar array deployed
Fairing needed	5-m or possibly 4-m	4-m	4-m
Launch vehicle required (minimum) for C_3 26.5 km^2/s^2	Atlas V (531) or Atlas V (431)	Atlas V (421)	Atlas V (421)

18. Summary of Major Mission and Spacecraft Trade Studies

The major IHS trade studies are summarized in **Table A-7**. Most of the listed studies were presented in more detail in the preceding sections of Appendix A or in Chapter 4.

Table A-7. Summary of major IHS trade studies.

Issue	Trade Space	Selection	Primary Rationale
Spin axis orientation	a. Orbit normal b. Sun pointed	Orbit normal (essentially ecliptic north)	Only orbit normal satisfies science requirements.
Spin rate	1 to 25 rpm	20 rpm	Satisfies science and thermal requirements.
Minimum perihelion distance	0.20 to 0.35 AU	0.25 AU	Solar array area and spacecraft mass and volume greatly increase at perihelion distances under 0.25 AU.
Most favorable balance between spacecraft downlink capability and DSN pass time to return the required volume of science data	a. Robust spacecraft downlink capability, reduced DSN pass time b. Less capable spacecraft downlink capability, additional DSN pass time	Robust spacecraft downlink capability, reduced DSN pass time	A constellation of four spacecraft could tax DSN capabilities (and become costly) if overly reliant on downlink time to return science data; the baseline spacecraft downlink capability can return all science data with one 8-hour pass per week per spacecraft.
Primary structure	a. Isogrid aluminum panels b. Thin-walled cylinder	Isogrid aluminum panels	Removable panels permit installation of propulsion subsystem by subcontractor and provide access to spacecraft interior during I&T.
Mechanical configuration of inter-spacecraft spacer cylinders	a. Incorporate cylinders into bottom of each spacecraft structure b. Jettison cylinders	Jettison cylinders	Incorporated cylinders block radiators and the aft LGA, and cause solar heating of the spacecraft.

Table A-7. Summary of major IHS trade studies (continued).

Issue	Trade Space	Selection	Primary Rationale
Launch configuration	a. Radial b. Stacked	Stacked	Radial requires a deployed solar array; is not a major axis spinner at separation; and requires a complicated launch vehicle adapter. Stacked configuration is simpler and lower risk.
Solar array and HGA configuration	a. Fixed b. Deployed	Fixed	Simpler, lower-risk spacecraft.
Solar array tilt angle	0° to 45°	45°	Optimal for radiator effectiveness, solar array temperature, and power generation.
Downlink frequency	a. X-band b. Ka-band	X-band	An X-band system is simpler than a Ka-band system and can return the required science data. A Ka-band system has tighter pointing requirements that would require a star tracker to be added to the G&C subsystem. Accommodation of a star tracker would be difficult (e.g., accommodating FOV, additional mass) and expensive.
HGA technology	a. Parabolic dish b. Parabolic wire cylinder c. Electronically scanned phased array d. Mechanically scanned phased array	Mechanically scanned phased array	Low mass, volume, and risk; the HGA gimbal does double duty by both deploying and pointing the HGA.
Location of RF components	a. Despun platform b. Spacecraft body	Spacecraft body	Superior thermal design; transmitter power can be increased; lower mass.
Number of transmitter power levels	One to three power levels	Two power levels	The medium-power transmitter is sized to support the emergency mode link; the high-power transmitter utilizes the increase in solar array output as the solar distance decreases; there is negligible benefit from a third transmitter.
High-power transmitter RF output power level	37 to 125 W	100 W	100-W transmitter maximizes science data return without requiring an increase in solar array size; thermal analysis shows that a 100-W transmitter can be accommodated.
Mission redundancy	a. Four spacecraft with redundant systems b. Five spacecraft with nonredundant systems	Four spacecrat with redundant systems	A nonredundant spacecraft is only ~5% lower in mass than a redundant spacecraft, so the mass of four redundant spacecraft is much less than the mass of five nonredundant spacecraft.
Spacecraft redundancy	a. Single string b. Partial redundancy c. Full (use redundant components or components with fault tolerance)	Full	Full redundancy necessary to satisfies 3-year lifetime requirement and 5-year lifetime goal
Mitigation of spin axis precession due to CM–CP offset	a. Thrusters b. Movable mass or solar sail	Thrusters	Only 1 kg of propellant is required to correct a 10 cm CM-CP offset for a 5-year mission.
Accommodation of growth in payload power beyond 30% of CBE	a. Increase solar array area b. Decrease solar distance that entire payload is turned on	Decrease solar distance that entire payload is turned on	Spacecraft design can power the entire payload at a solar distance of 0.88 AU with 30% payload power margin.

Appendix B: Inner Heliospheric Sentinels Mass and Power Estimates

Table B-1: Mass estimates.

Component	Mass (kg)
Instruments	
Dual Magnetometer	0.5
Dual Mag Boom	10.0
SW Electrons	1.5
Search Coil	0.5
SW/SC Boom	5.0
Protons/Alpha	4.0
Composition	6.0
Radio	4.7
Low Energy Ions	3.5
High Energy Ions and electrons and Boom	8.0
SEP Q-States and SEP DPU	10.5
Energetic Electrons & Suprathermals	2.0
Neutron Spectrometer	3.8
XR Imager	2.0
Gamma Spectrometer	2.2
Common DPU	3.0
DPU components	1.8
Purge system	0.1
Instrument harness	1.4
Instruments subtotal	70.5
Attitude Determination and Control	
Star scanner (2)	8.2
Accelerometers (2)	2.0
Sun sensors (2)	2.5
Attitude subtotal	12.7
Command & Data Handling	
IEM & OCXO -A	5.6
IEM & OCXO -B	5.6
Command subtotal	11.2
Power	
Solar arrays	41.6
Solar array hinges/brackets	5.1
Power distribution unit	14.0
Power system electronics	8.6
Junction box	1.5
Battery	10.0
Power subtotal	80.7
Structure	
Honeycomb decks and fasteners, average mass	57.7
Load-bearing structure, average mass	69.7
Despun platform	7.3
RF radiators with mounts	1.9
Secondary structure	9.7
Fasteners	2.3
Spin balance mass (no Cg offset)	13.0
Structure subtotal	161.6

Component	Mass (kg)
Propulsion	
Propellant tank (2)	7.4
Thrusters 4.4N (12)	4.8
Latch and service valve	1.3
Propellant filter	0.4
Pressure transducer	0.8
Cabling and connectors	3.4
Tubing/fasteners/tube clamps/etc.	5.1
Propulsion subtotal	23.2
RF Communications	
HGA	4.9
RF support structure	4.6
BAPTA & Electronics Box	20.9
HGA Actuator	2.3
Forward LGA and MGA	0.9
Aft LGA and boom	11.1
Rotary joints (2)	3.5
TWTA (4)	9.2
Transponder (2)	6.0
Waveguide RF Transfer Switches (3)	2.0
Waveguide diplexer (2) and Isolators (4)	2.0
Radome, pressure baffle, support	3.4
Waveguide runs	1.2
Coax transfer switch, filters	1.2
RF subtotal	73.1
Thermal	
MLI blankets	5.0
Radiator	4.0
Thermal curtains	0.5
OSRs	5.2
OSR Panels	5.4
Louvers	5.0
Despun thermal spacer	0.3
Heaters and miscellaneous	0.1
Thermal subtotal	25.5
Harness	
S/C harness, 9% dry mass	45.3
Harness subtotal	45.3
Spacecraft dry mass total (average)	**503.7**
Launch	
Wet mass with margin (average)	697.8
Usable propellant	42.5
Trapped propellant and pressurant	0.5
Dry mass with margin (average)	654.8
Dry mass with margin (top spacecraft)	614.1
Dry mass with margin (bottom spacecraft)	695.9
Margin on dry mass (average), kg	151.1
Margin on dry mass %	30.0%
Bottom spacecraft wet with margin	738.9
Mid-Lo spacecraft wet with margin	709.2
Mid-Hi spacecraft wet with margin	686.3
Top spacecraft wet with margin	657.1
Mass of 4 observatories	2791.3
Jettisoned support cylinders w/ 30% margin	89.0
Separation and jettison systems w/ 30% margin	312.0
Total Launch Mass	**3192.4**

Table B-2: Power estimates.

Subsystem/Component	Average Power (W)				
	Launch Configuration	Platform Off, Instr. Off, Med-Pwr Downlink On	Platform On, Instr. Off, Med-Pwr Downlink On	Platform On, Instr. On, Med-Pwr Downlink On	Platform On, Instr.On, High-Pwr Downlink On
Instruments					
Dual Magnetometer	0.0	0.0	0.0	1.0	1.0
SW Electrons	0.0	0.0	0.0	1.5	1.5
Protons/Alpha	0.0	0.0	0.0	4.0	4.0
Composition	0.0	0.0	0.0	6.0	6.0
Radio	0.0	0.0	0.0	3.0	3.0
Search Coil	0.0	0.0	0.0	0.2	0.2
Low Energy Ions	0.0	0.0	0.0	3.0	3.0
High Energy Ions and Electrons	0.0	0.0	0.0	5.0	5.0
SEP Q-States	0.0	0.0	0.0	4.0	4.0
SEP DPU	0.0	0.0	0.0	6.5	6.5
Energetic Electrons and Suprathermals	0.0	0.0	0.0	2.0	2.0
Neutron Spectrometer	0.0	0.0	0.0	3.0	3.0
XR Imager	0.0		0.0	2.0	2.0
Gamma Spectrometer	0.0		0.0	0.5	0.5
Common DPU	0.0		0.0	3.3	3.3
Instruments subtotal (assume 65% conv eff)	0.0	0.0	69.0	69.0	
Attitude Determination and Control					
Star scanner—power provided by IEM	0.0	0.0	1.0	1.0	1.0
Accelerometers (3)—power provided by IEM	0.0	0.0	0.0	0.0	0.0
Sun sensor	0.0	0.0	1.0	1.0	1.0
Attitude subtotal	0.0	0.0	2.0	2.0	2.0
Command & Data Handling					
IEM A (includes OCXO)	21.0	21.0	21.0	24.0	24.0
IEM B	3.0	3.0	3.0	3.0	3.0
IEM subtotal	24.0	24.0	24.0	27.0	27.0
Power					
Power distribution unit	18.0	18.0	18.0	18.0	18.0
Power system electronics	6.0	6.0	6.0	6.0	6.0
Solar array junction box	0.0	0.0	0.0	0.0	0.0
Battery recharge	0.0	20.0	20.0	20.0	20.0
Power subtotal	24.0	44.0	44.0	44.0	44.0
Propulsion					
Thrusters - assume 2 x 1 lb thrusters	0.0	0.0	0.0	0.0	0.0
Cat bed heaters—4 for launch, 2 for maneuvers	16.0	0.0	0.0	0.0	0.0
Pressure sensors (4 at 0.9 W each)	3.6	3.6	3.6	3.6	3.6
Propulsion subtotal	19.6	3.6	3.6	3.6	3.6

Table B-2: Power estimates. (Cont.)

Subsystem/Component	Average Power (W)				
	Launch Configuration	Platform Off, Instr. Off, Med-Pwr Downlink On	Platform On, Instr. Off, Med-Pwr Downlink On	Platform On, Instr. On, Med-Pwr Downlink On	Platform On, Instr.On, High-Pwr Downlink On
RF Communications					
Receiver A	5.6	5.6	5.6	5.6	5.6
Receiver B	5.6	5.6	5.6	5.6	5.6
Exciter	0.0	4.0	4.0	4.0	4.0
Med/high power transmitter	0.0	50.0	50.0	50.0	200.0
BAPTA & BAPTA Electronics	0.0	13.5	13.5	13.5	13.5
HGA actuator	0.0	3.0	3.0	3.0	3.0
RF subtotal	11.2	65.2	81.7	81.7	231.7
Thermal					
Thruster valve heaters (12 @2.2 W each)	8.8	26.4	26.4	26.4	26.4
Fuel line heaters (0.1 W per foot)	0.0	4.0	4.0	4.0	4.0
Fuel tank heater	0.0	10.0	10.0	10.0	10.0
Instrument operational heaters	0.0	0.0	0.0	0.0	0.0
Instrument survival heaters (need when instr off)	0.0	20.0	20.0	0.0	0.0
Battery heater	0.0	7.5	7.5	7.5	7.5
Thermal subtotal	8.8	67.9	67.9	47.9	47.9
Harness					
IR loss (1.5% of load power)	1.3	3.1	3.3	4.1	6.4
Total Current Best Estimate (CBE)	88.9	209.8	226.5	279.4	431.6
Total CBE Plus 30% Margin	115.6	272.7	294.5	363.2	561.1

Appendix C: Inner Heliospheric Sentinels Spacecraft and Launch Stack Dimensions and Mechanical ICD

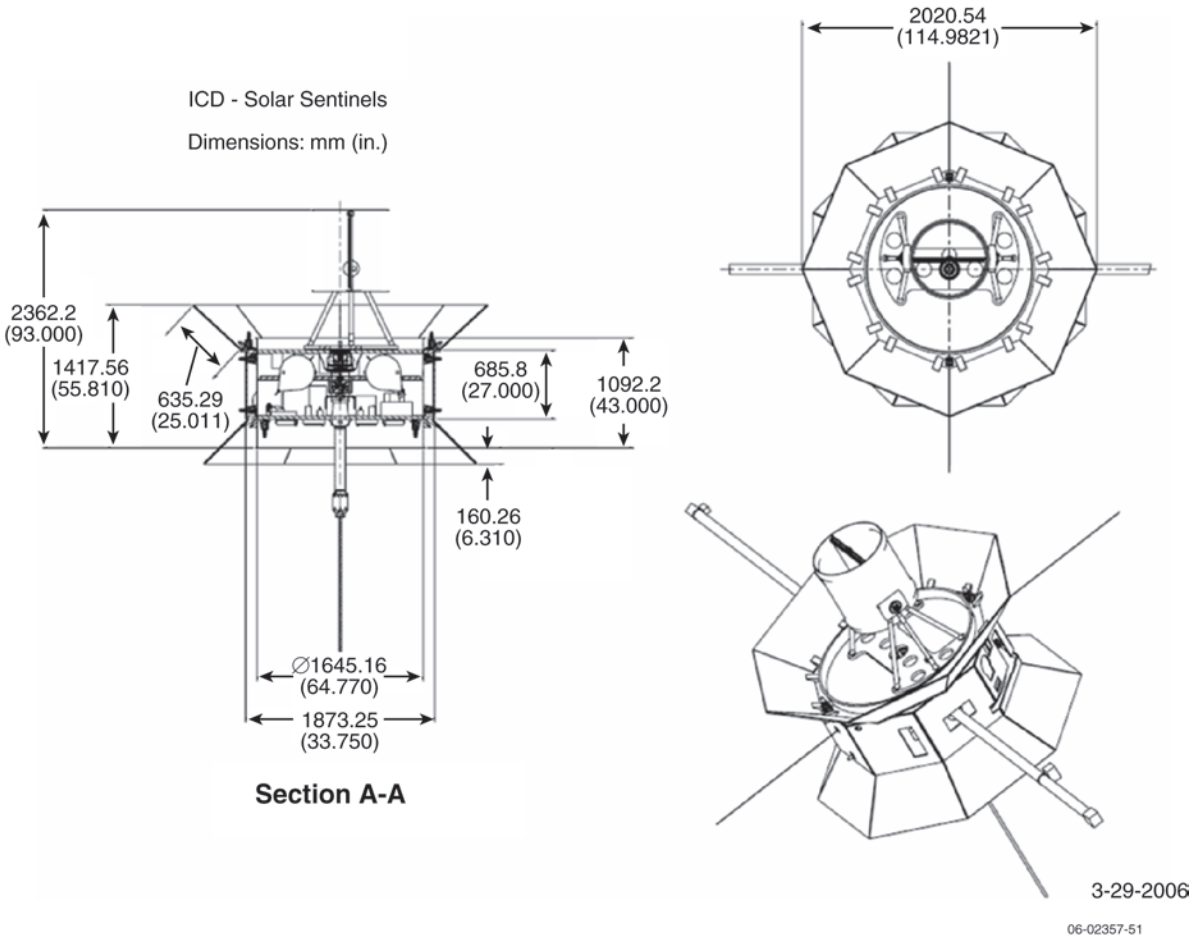

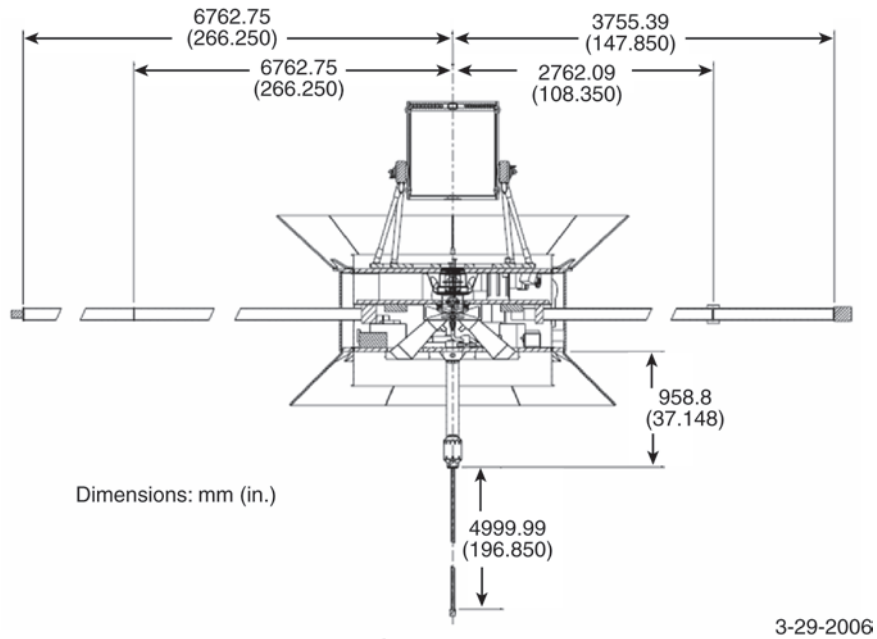
6762.75
(266.250)
3755.39
(147.850)
6762.75
(266.250)
2762.09
(108.350)
958.8
(37.148)
Dimensions: mm (in.)
4999.99
(196.850)
3-29-2006
Section B-B
06-02357-52

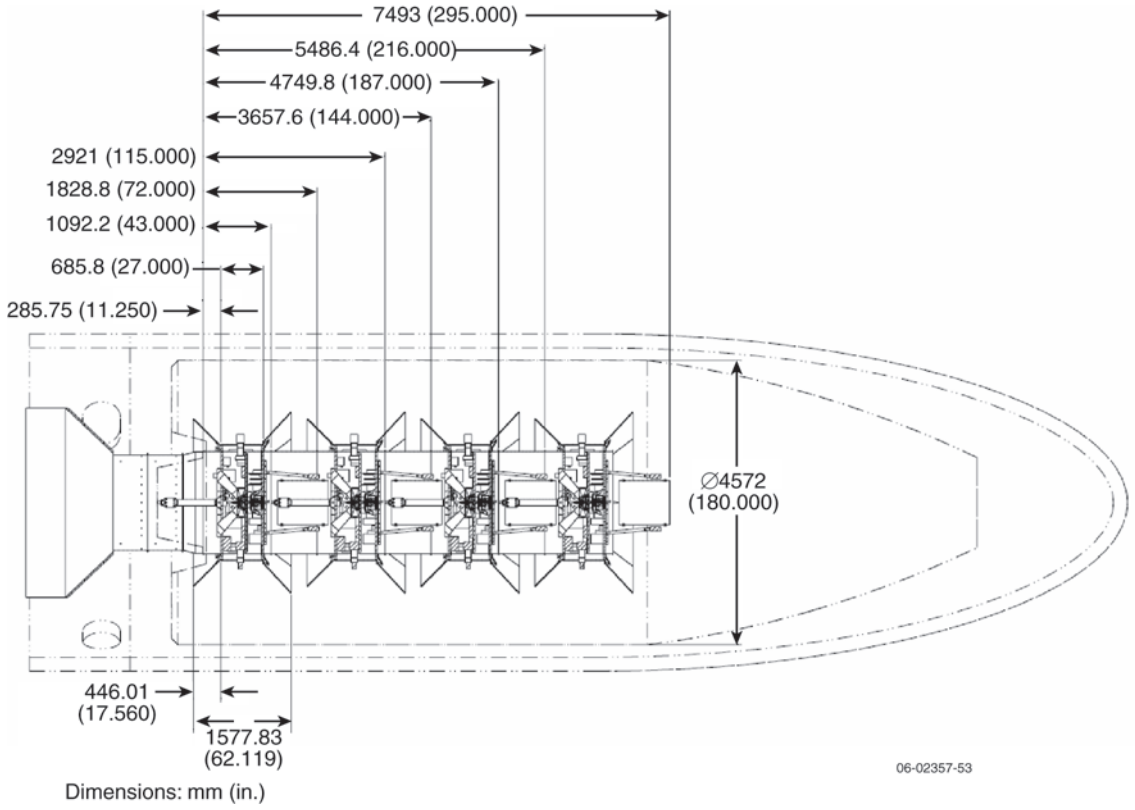
7493 (295.000)
5486.4 (216.000)
4749.8 (187.000)
3657.6 (144.000)
2921 (115.000)
1828.8 (72.000)
1092.2 (43.000)
685.8 (27.000)
285.75 (11.250)
Ø4572
(180.000)
446.01
(17.560)
1577.83
(62.119)
06-02357-53
Dimensions: mm (in.)

Appendix D: Farside Sentinel: Report of the Science and Technology Definition Team

The Farside Sentinel (FSS) is designed to complement the Inner Heliospheric Sentinels (IHS) mission, which is tasked with probing the characteristics of the solar environment to within 0.3 AU of the Sun. While the four IHS spacecraft will conduct detailed in-situ investigations, FSS will provide a global context for these local measurements by studying the Sun from near 1.0 AU in conjunction with observations from the Earth. Thus, the more comprehensive view provided by the FSS mission will contribute to an improved understanding of the overall solar dynamics.

This section provides a high-level summary of the work completed in support of the Sentinels Science and Technology Definition Team (STDT). This summary is divided into two principal areas, as outlined below. Section D.1 provides an overview of the major design drivers and the overall mission trade space, and Section D.2 reviews a specific point design that fulfills the mission objectives consistent with a six-instrument suite. Additionally, a one-instrument design (using only the magnetograph) is presented as a comparison and possible "floor" option.

The geometry of the FSS mission is outlined in **Figure D-1**, which shows an ecliptic view of the mission. A single spacecraft would be placed into an Earth-leading orbit (~1 AU heliocentric range) that provides solar visibility from 60° to 180° ahead of the Earth. Additionally, a second spacecraft (nearly identical to the first) may be launched into an Earth-trailing orbit. Although this latter option was not studied, the major design drivers and spacecraft design presented in this section would generally apply to both the leading and trailing spacecraft with small design changes and less development risk for the second spacecraft.

One of the principal mission requirements is to provide overlap with the science phase of the IHS mission. The IHS mission was studied in parallel to this report, requiring several assumptions. It is assumed for this section that the earliest IHS launch would occur in January of 2014. IHS cruise would last 1 year followed by 4 years of science operations. Furthermore, the earliest FSS launch would occur in 2016 (2 years after the IHS launch), allowing a maximum overlap with the IHS mission of 3 years.

D.1 Major Design Drivers

The FSS system design is driven by the science objectives, as identified by the STDT. In particular, the instrument payload and trajectory have a major impact on the design. Depending on the instrument suite, its development can be nearly as complex and labor intensive as the spacecraft bus. Part of this complexity is due to the addition of the guide telescope, which is required by several instruments and imposes a need for precise pointing knowledge. The other principal driver is the set of derived requirements from the trajectory. The trajectory design process endeavors to fulfill the viewing requirements, including overlap with IHS, while trading launch vehicle size, flight times, magnitude of ΔV, and type of propulsion. The requirements derived from this process drive the use of a redundant spacecraft design (due to a longer flight time) and a more capable launch vehicle. Combined, the instrument payload and trajectory design directly drive the majority of the mission budget.

A secondary design driver is the science collection data rate. This data rate may fluctuate between 37.3 and 500 kbps, depending on desired science. While the data rate was found to be a less influential system driver, it is included in this analysis given the general desire to collect additional science data.

Table D-1 presents a summary of the principal design drivers, including the baseline used for this report, other options considered, and the type of analysis employed. The primary mission driver is

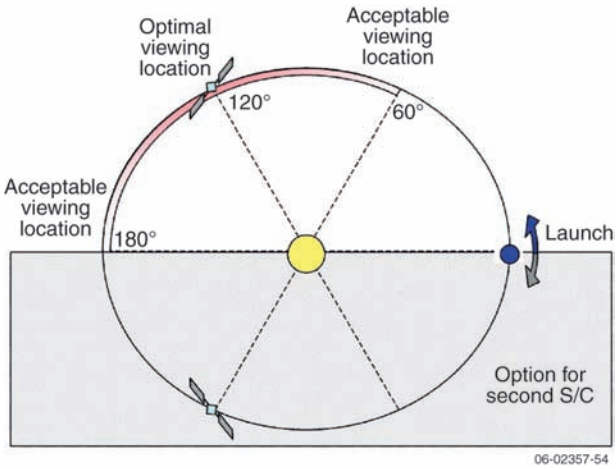

Figure D-1. Imaging Sentinels mission overview.

Table D-1. Summary of major design drivers.

Design Driver	STDT Report	Other Options	Type of Analysis
1. Instrument payload	Six-Instrument Suite: Magnetograph + Coronagraphs + In Situ	• Magnetograph only • Helioseismology • Magnetograph and Coronagraphs	Point designs system trade studies
2. Trajectory	0° to 180° drifting with lunar gravity assists	• 120° Fixed • Optimal 60° to 180° • 0° to 180° drifting (slow) • 0° to 180° drifting (fast)	Trajectory analysis system trade studies
3. Science data collection rate	115.6 kbps	• 37.3 to 500 kbps	Telecom analysis system trade studies

the instrument payload, which offers the greatest flexibility in reducing mission complexity. While the six-instrument suite studied in this report would be ideal, descoping to a one-instrument option would provide significant savings. Additionally, the trajectory provides an opportunity to trade mission complexity with the orbit location and duration of IHS overlap. Although a 0° to 180° drifting orbit is suboptimal for science collection, it allows a smaller Taurus launch vehicle to be used. Finally, the data rate may be varied from 37.3 to 500 kbps, depending on the desired science and available launch vehicle margin.

D.1.1 Science objectives. There are four instrument options that were identified by the STDT and considered here as part for the FSS mission trade space. These four options are outlined below and collectively build on each other. The minimum mission would be a simple magnetograph mission, whereas an ideal mission would be the magnetograph, two coronagraphs, and a package of in-situ instruments.

- ***Magnetograph***—Map the photospheric magnetic field from a different heliospheric longitude than Earth.
- ***Helioseismology—***Map the photospheric magnetic field from a different heliospheric longitude than Earth; also, provide Doppler measurements to allow helioseismology studies.
- ***Magnetograph + Coronagraphs***—Map the photospheric magnetic field from a different heliospheric longitude than Earth; also, observe coronal mass ejection (CME) propagation, high-speed streamers, electron jets, and other coronal structures from the solar surface to 60 R_S.
- ***Magnetograph + Coronagraphs + In Situ*** — Map the photospheric magnetic field from a different heliospheric longitude than Earth, observe CME propagation, high-speed streamers, electron jets, and other coronal structures from the solar surface to 60 R_S; also, measure the in-situ plasma, magnetic field and energetic particle populations.

An instrument summary of these options is included in **Table D-2**. The table illustrates the instrument suite for each option. The first six instruments are science instruments, whereas the last two (the guide telescope and electronic boxes) are engineering components. Although a suggested data rate is listed below each option, this rate is flexible (that is, more is better), making it a separate design consideration.

D.1.2 Trajectory objectives. To be at the desired location at the right time for science data acquisition is a critical design driver. Attaining an orbit with the necessary Earth-relative phasing requires considerable cruise time and/or a larger launch vehicle. While there is some flexibility in the trajectory design, the resulting minimum acceptable mission duration is in excess of 3 years, requiring the use of redundancy in the flight system design. Similarly, escaping Earth's gravity requires more capability from the launch vehicle. Preferred trajectories (fully responsive to science desires) require the use of a Delta II launch vehicle. However, using trajectories with suboptimal flight path characteristics and/or minimizing the payload allow the use of a less costly Taurus launch vehicle.

Four trajectory options are presented in **Figure D-2**. They are selected as examples because they present performance suitable across several categories of requirements, including solar viewing positioning, overlap with IHS, and launch mass capability. Key mission parameters are presented in this table, illustrating how mission drivers (such

Table D-2. Summary of instrument options.

Instrument	Magneto-graph	Helio-seismology	Magnetograph + Coronagraphs	Magnetograph + Coronagraphs + In Situ (STDT Report)
Magnetograph	X		X	**X**
Enhanced Magnetograph		X		
Inner Coronagraph			X	**X**
Outer Coronagraph			X	**X**
Magnetometer				**X**
Solar Wind Proton & Electron				**X**
SEP Telescope				**X**
Guide Telescope			X	**X**
Electronic Boxes			X	**X**
Total mass	5.0 kg	7.0 kg	48.0 kg	**66.5 kg**
Total power	4.0 W	8.0 W	115.0 W	**130.0 W**
Total data rate	37.3 kbps	158.0 kbps	111.9 kbps	**115.6 kbps**

as ΔV and flight time) may be traded. Additionally, a fifth option is discussed, which is a derivative of the other trajectories, but includes two lunar gravity assists to increase the launch mass injection capability.

- ***120° fixed***—This trajectory design is driven by the desire to place a spacecraft in an Earth-relative fixed location (120° Earth-leading) as fast as possible, while delivering a suitable science payload.
- ***Optimal 60° to 180° drifting***—This option maximizes the overlap time with IHS by increasing the cruise time to reach 60° Earth-leading, and then slowing the drift rate to match the remaining IHS mission duration.
- ***0° to 180° drifting (slow)***—This option minimizes the post-launch ΔV to allow the use of a smaller

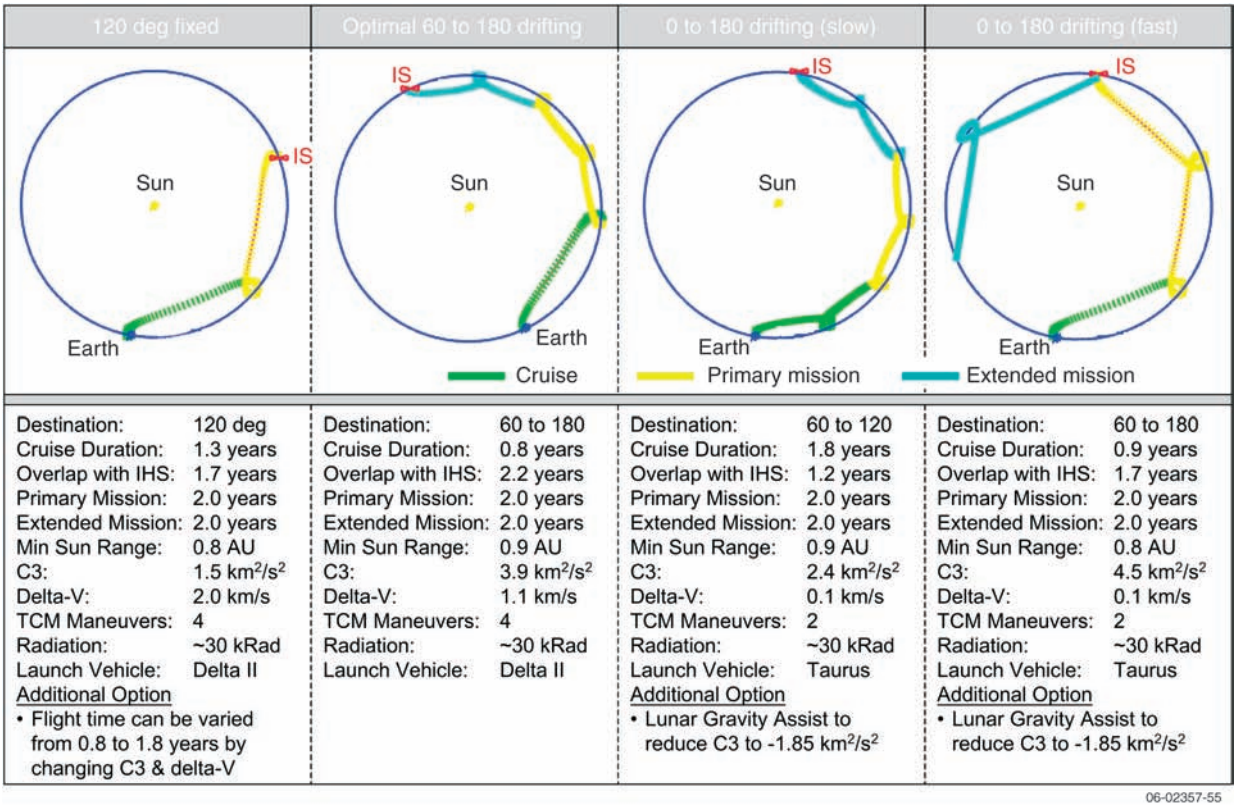

Figure D-2. Summary of trajectory options.

launch vehicle. The trajectory drifts slowly from Earth to the far side of the Sun over 6 years, which includes cruise, primary operations, and extended operations.

- ***0° to 180° drifting (fast)***—Like to the preceding option, this trajectory minimizes the post-launch ΔV, but the drift rate is faster, allowing the spacecraft to reach the far side of the Sun at the end of primary operations.
- ***0° to 180° drifting with two lunar gravity assists***—This option is a derivative of the third option, but includes two lunar gravity assists (LGAs). The LGAs lower the launch vehicle capability requirement (C3), but extend the cruise time.

D.1.3 Data acquisition strategy. Although the data rate is not a primary design driver, increases in data rate require the tailoring of the given flight system design to arrive at an optimal solution. Increasing or decreasing the data acquisition rate will drive the mass of the telecommunications and power subsystems. For the given options studied and depending on the launch vehicle margin, the data rate can sometimes be increased to use excess launch capability.

In general, the optimization method is to adjust the telecom/ground-system design for a given data rate while staying within the selected launch vehicle performance range. The transmitter size, high gain antenna (HGA), length and number of weekly Deep Space Network (DSN) passes, and DSN array are traded, emphasizing reduced mission operations, low flight system mass, and/or limited volume availability. For example, to accommodate a 500 kbps data rate and a Taurus launch vehicle, a 1.25 m HGA, two 8-hour passes/week, and 100 12-m DSN nodes are required. **Table D-3** summarizes the scope of the optimization parameters investigated.

D.1.4 Other design considerations. Beyond the principal design drivers, many other subsystem trades were considered, which contributed positively to the overall design. Of these trades, the attitude control (ACS) and propulsion subsystem trades are critical design considerations and are addressed in this subsection.

For this mission, there are three types of potential propulsion systems: monopropellant, bipropellant, and solar electric propulsion (SEP). Of these, monopropellant is the cheapest, but least efficient (Isp = 225 s). Bipropellant is slightly more expensive and more efficient (Isp = 325 s), and finally SEP is very expensive and highly efficient (Isp = 3100 s). Thus, a trade study was performed to determine what, if any, benefit might be realized from these three propulsion systems. The result was that a monopropellant system offers nearly equivalent performance at a lower price for all of the options considered.

Another trade study was conducted to determine what type of ACS system would provide the desired pointing and stabilization precision. The two primary options, both of which require the guide telescope pointing knowledge, were reaction wheels and warm-gas thrusters. The reaction wheels provide exceptional performance, but they are heavy and complex. In contrast, the warm-gas thrusters are a simpler solution. The result of this analysis showed that a warm-gas thruster system is feasible, which would significantly reduce mass and complexity. Additionally, the magnetograph, instead of the guide telescope, could provide the necessary pointing knowledge.

D.1.5 Mission trade space. To establish the mission trade space available within the constraints, three activities were conducted in parallel: (1) four "end-to-end" point designs were completed by the study team, (2) individual trajectory and subsystem trades were evaluated, and (3) the results were used to iteratively populate the Systems Trade Model (STM). The STM is a tool that models the payload, trajectory, subsystem, and ground system inputs. Once subsystems have been defined, characterized, and populated by the study team, the tool can

Table D-3. Summary of data rate options.

Science Data Rate Options	Telecom Subsystem Design & Ground Systems (optimized for design)			
	Transmitter Size	High Gain Antenna	Weekly Passes	DSN Coverage
37 to 500 kbps	25 to 250 W TWTA	0.85 to 1.5 m	4 to 8 hour duration 1 to 2 passes/week	36 to 100 12-m nodes (assumes new 200 node 12-m DSN array)

approximate alternative designs that are similar in nature to the existing point designs, modeling the downstream interactions and providing a trade space of insights. For this study, a trade space of hundreds of potential mission permutations was identified. Each permutation includes a mass equipment list, power budget (for three modes), and cost per element of the work breakdown structure (WBS), albeit additional validation is required to further consider individual options.[1]

In this context, the STM was used to support the FSS study. Specifically, the major design drivers were varied to produce an array of supporting mass, power, and schedule information. **Figure D-3** explicitly shows the impact from the four instrument options. The first and last options are based on point designs generated by the flight system team, whereas the middle options are an STM product. The result shows that the payload mass directly drives the flight system mass. More specifically, only the payload, structure, and cabling mass vary across the increasingly complex payload options. In contrast, the mass of the other subsystems remains nearly constant. As the options vary, component selections are adjusted within the power, attitude control, thermal, and telecom subsystems.

[1]Rather than validated point designs, the tool results are simply a guide for determining options for further study.

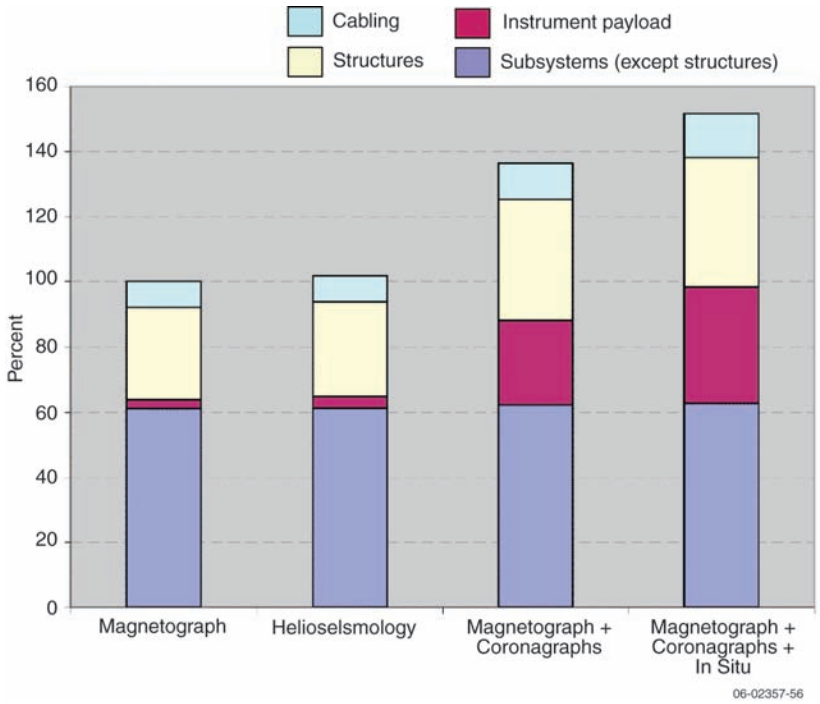

Figure D-3. Impact of instrument options on spacecraft dry mass.

Similarly, the modeling tool was used to consider mission launch mass with respect to payload, trajectory, and data rate. The results are shown in **Table D-4**, which provides a comprehensive understanding of the mission trade space. The matrix consists of the five trajectory options, four payload options, and two data rate options, resulting in 40 unique design concepts. These concepts are listed by total launch mass and color-coded by the approximate mission proposal class. Additionally, three of the point designs that were used to span this trade space are outlined in bold.

D.2 Mission Implementation: Six-Instrument Taurus Option

The science objectives for the Imaging Sentinel suggest a variety of mission concepts, which were examined in the previous section as part of the comprehensive mission trade space. Of these missions, the Six-Instrument Taurus Option was selected for this section. It is a point design (developed by the engineering study team), includes a full instrument suite, and fits on a Taurus launch vehicle. It uses a 0° to 180° drifting trajectory and a data rate of 115.6 kbps. Additionally, a second concept, the One-Instrument Taurus Option, is summarized as a comparison to the baseline mission. This second concept (also developed by the study team) is a point design that provides a simpler solution and satisfies the floor science requirements.

D.2.1 Instrument definition. The baseline mission concept includes six science and two engineering instruments, as defined by the STDT, which are characterized in **Table D-5** and **Table D-6**, alongside the One-Instrument Taurus Option. This instrument suite includes a magnetograph, inner and outer coronagraphs, magnetometer, solar wind proton and electron telescope, and solar energetic particle (SEP) telescope, along with the guide telescope and the camera and electronic boxes. This combined instrument suite provides the following capabilities:

Table D-4. Mission trade space.

Trajectory Options	Total Launch Mass (kg) Instrument Payload Options: Magnetograph	Helioseismology	Magnetograph + Coronagraphs	Magnetograph + Coronagraphs + In situ
120° fixed	L: 510 kg	H: 580 kg	H: 737 kg	H: 765 kg
	VL: 458 kg	L: 517 kg	L: 674 kg	L: 742 kg
Optimal 60° to 180° drifting	L: 479 kg	H: 545 kg	H: 693 kg	H: 719 kg
	VL: 429 kg	L: 485 kg	L: 633 kg	**L: 697 kg (3)**
0° to 180° drifting (slow)	L: 273 kg	H: 328 kg	H: 357 kg	H: 429 kg
	VL: 243 kg	L: 276 kg	L: 349 kg	L: 370 kg
0° to 180° drifting (fast)	L: 273 kg	H: 328 kg	H: 349 kg	H: 429 kg
	VL: 243 kg (1)	L: 276 kg	L: 349 kg	L: 394 kg
0° to 180° drifting w/LGA	L: 273 kg	H: 328 kg	H: 394 kg	H: 395 kg
	VL: 243 kg	L: 276 kg	L: 364 kg	**L: 402 kg (2)**

Validated point designs

(1) One-Instrument Taurus Option	**Mission cost**	**MIDEX class**			**Discovery class**
(2) Six-Instrument Taurus Option		VL	L	M	H / VH
(3) Six-Instrument Delta II Option	**Data rate**	VL = 37.3 kbps	L =115.6 kbps		H = 500 kbps

Table D-5. Instrument payload overview.

Payload	Six-Instrument Taurus Option	*One-Instrument Taurus Option*[a]
Number of science instruments	6	*1*
Number of engineering instruments	2	*0*
Mass	66.5 kg	*5.0 kg*
Power	130.0 W	*4.0 W*
Science data collection rate	115.6 kbps	*37.3 kbps*

[a] The One-Instrument Taurus Option includes only the Magnetograph, which fulfills the first science capability of measuring the surface structure, solar dynamics, and solar magnetic flux.

Table D-6. Detailed instrument specifications.

Instruments	Mass (kg)	Power (W)	Data Rate (kbps)	Comments
Magnetograph	10.0	20.0	37.3	Unique magnetographs are used for each design
Inner Coronagraph	10.0	20.0	37.3	Pointing requirements: 20 arcsec control, 0.1 arcsec knowledge, <5 arcsec/s stability
Outer Coronagraph	10.0	20.0	37.3	
Magnetometer	2.5	1.0	0.5	Requires a 5-m boom
Solar Wind Proton & Electron	6.0	6.0	2.0	
SEP Telescope	10.0	8.0	1.2	
Guide Telescope	3.0	5.0	–	Engineering instrument, which provides 0.1 arcsec pointing knowledge
Camera & Electronic Boxes	15.0	50.0	N/A	Includes an instrument data processing unit (IDPU)
Total	**66.5**	**130.0**	**115.6**	

- Map the photospheric mag-netic field from a different heliospheric longitude than Earth
- Observe CME propagation, high-speed streamers, electron jets, and other coronal structures from the solar surface to 60 R_S
- Measure the in-situ plasma, magnetic field and energetic particle populations.

Table D-6 provides a detailed summary of the instrument specifications. It outlines the mass, power, and data rate specifications for the payload. Additionally, this table provides some information on the pointing requirements. Specifically, the inner and outer coronagraphs drive the pointing requirements. They require 20-arcsec control from the

spacecraft to locate the Sun-center. Once located, a pointing knowledge of 0.1 arcsec (provided by the guide telescope) is required along with stability of better than 5 arcsec/s. These fine pointing requirements and the complex interaction between the instrument suite and the attitude control subsystem require some atypical payload elements. First, the instruments should be mounted as an integrated payload module on a carbon optic bench, as they require careful alignment and integration. Second, an instrument data processing unit (IDPU) is required to coordinate data transfer with the guide telescope. This component is included in the electronic boxes. Finally, the magnetometer requires a 5-m boom in order to provide some separation from the spacecraft.

In the case of the One-Instrument Option, the payload is significantly reduced. The pointing requirements are relaxed such that the star cameras, Sun sensors and inertial measurement unit (IMU) can provide adequate pointing control and knowledge (eliminating the need for the guide telescope) and, similarly, the IDPU is unnecessary. The Magnetograph provides its own internal mechanization for jitter control.

D.2.2 Mission design. Reaching the far side of the Sun is on par with interplanetary travel. Consequently, the trajectory for this mission is a design driver. Several possible trajectories were investigated, including fixed orbits, drifting orbits, varying rates of speed, low-energy trajectories, and lunar gravity assists (LGAs). Of these, the 0° to 180° Drifting Orbit with LGAs was selected for two reasons. It results in a relatively long overlap with IHS (1.5 years), while maintaining a sufficiently low C3 (–1.85 km^2/s^2) to accommodate a Taurus launch vehicle. With 30% mass and power contingency and 3σ ΔV load, this combination may raise the risk, as the resulting launch vehicle margin is low (that is, <10 kg). If the spacecraft grows beyond the design contingency, then either a Delta II launch vehicle would be required; alternatively, reoptimization of the flight system and data return strategy might allow launch within the Taurus performance. **Table D-7** lists additional parameters related to mission design, along with a comparison to the One-Instrument Taurus Option, which uses a similar trajectory, but without the LGAs.

0° to 180° drifting trajectory with lunar gravity assists. The trajectory chosen for the baseline mission concept is shown in **Figure D-4**. Following launch from Earth, the trajectory uses two unpowered LGAs to escape Earth's orbit. The trajectory then becomes a solar elliptical orbit (0.85 × 1.0 AU), which results in a drift velocity of 60° per year and provides 1.5 years of overlap with the IHS mission. The primary mission ends after 2 years of science, when the spacecraft reaches the far side of the Sun. Beyond this location, the spacecraft has the option of entering an extended mission phase, as the spacecraft continues beyond 180° leading. If a 2-year extended mission is approved, the spacecraft would reach 300° Earth-leading (or 60° Earth trailing) at the conclusion of the 5.5-year mission. Additionally, a preliminary estimate of navigational ΔV shows the 85 m/s would be sufficient for this trajectory. (The STEREO mission, with a similar trajectory, uses 100 to 180 m/s for ΔV, depending on the launch date.)

Launch vehicle performance. **Figure D-5** shows the launch vehicle performance for the most likely range of launch vehicles, given a C3 of –1.85 km^2/s^2. Data for this graph was generated from the

Table D-7. Mission design overview.

Mission Design	Six-Instrument Taurus Option	*One- Instrument Taurus Option*
Destination	0 to 180 Drifting	*0 to 180 Drifting*
Lunar gravity assist?	Yes (×2)	*No*
Duration of IHS overlap	1.5 years	*1.7 years*
Maximum Sun range	0.85 AU	*0.8 AU*
Maximum Earth range	2.0 AU	*2.0 AU*
C3	–1.9 km^2/s^2	*4.5 km^2/s^2*
ΔV	85 m/s	*85 m/s*
Number of maneuvers	6	*2*
Launch vehicle (LV)	Taurus 3113 / Star 37F	*Taurus 2130*
Fairing size (inner diameter)	1.4 m	*1.4 m*
LV adapter (LV-side) included?	No	*Yes*
LV performance	445.0 kg	*310.0 kg*
LV margin	8.7 kg	*67.3 kg*

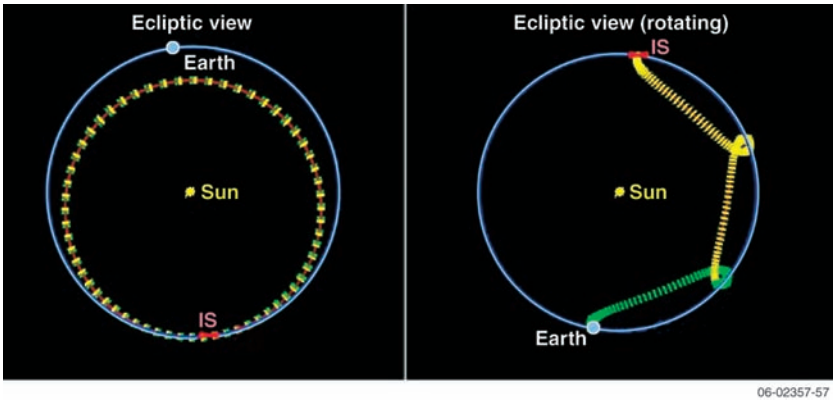

Figure D-4. 0° to 180° drifting trajectory with lunar gravity assists.

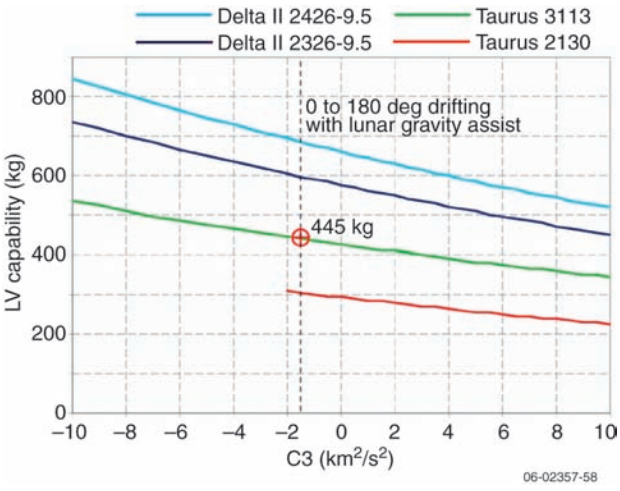

Figure D-5. Launch vehicle performance.

3113, adds a volume constraint within the fairing. Specifically, the fairing diameter is 1.4 m and the height (after providing for the Star 37 F motor) is 2.4 m. These constraints require a configuration design to ensure that adequate volume margin exists with the proposed mission concept. **Figure D-6** shows how this configuration works, along with the necessary design changes to accommodate this concept. The principal change was to the high gain antenna, which decreased from 1.5 m (on the Delta II) to 1.25 m to accommodate the smaller Taurus diameter. Additionally, deployment mechanisms were added to the four solar array panels, allowing them to be stowed during launch. Also shown in the figure below are the fourth and fifth stages of the Taurus 3113. The fourth stage is an Orion motor, and the fifth stage is the Star 37 F motor, which is housed within the payload fairing.

D.2.3 Flight system overview. FSS requires an interplanetary, dual-redundant flight system design that can accommodate a 66.5 kg and 130 W payload on a trajectory to the far side of the Sun. These requirements limit the potential use of an off-the-shelf industry spacecraft. Instead, a flight system

Kennedy Space Center (KSC) Launch Vehicle Site for the Delta II and Taurus 2130 options. However, for the Taurus 3113, unofficial estimates were used, given known launch vehicle parameters, combined with a Star 37 F solid rocket booster. Additionally, this capability (445 kg) does not include an adapter on the launch vehicle side (~30 kg), which has been accounted for separately in the mass equipment list.

Launch vehicle accommodation. The selection of a Taurus, particularly the Taurus

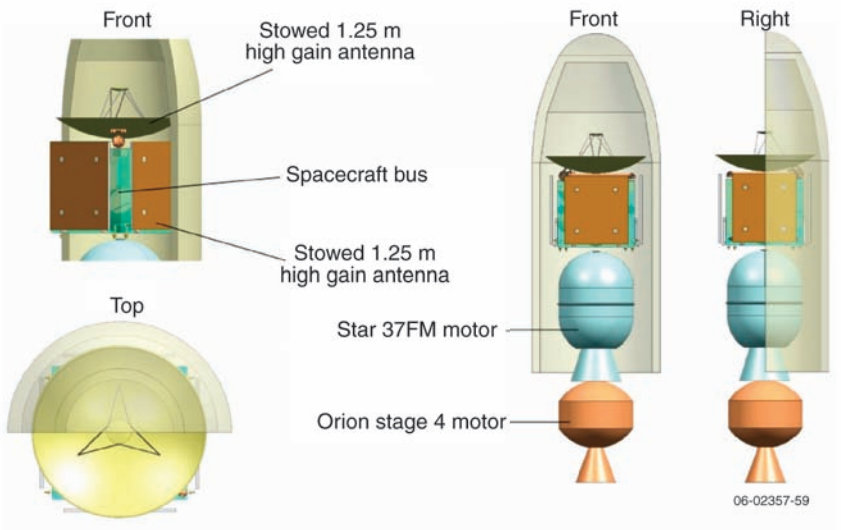

Figure D-6. Launch vehicle accommodation.

team generated a design that emphasizes available, high-heritage components, as outlined in this section.

Description. The key flight system parameters are listed in **Table D-8**. The spacecraft is an industry-subcontracted spacecraft with a lifetime of at least 3.5 years. It is primarily dual-string, except for specific components such as the high gain antenna and the instrument payload. It is radiation tolerant for an expected lifetime dose of 30 krad. It is cube-shaped with an aluminum honeycomb structure, four deployable solar arrays, a deployable high gain antenna, and a deployable 5-m boom for the magnetometer. The single internal hydrazine tank is located beneath the integrated instrument module.

The spacecraft dry mass is fairly light at 216.8 kg. However, once the payload, launch vehicle adapters, 30% contingency, and propellant are added, the total launch mass becomes 439.5 kg, which is just under the 445 kg launch vehicle capability. The peak power, including contingency, is 595.1 W, which is reached while operating the thrusters.

The spacecraft block diagram is shown in **Figure D-7**, which outlines the key spacecraft components. These components are further discussed as distinct subsystems in the following sections. In general, the

Table D-8. Flight system overview.

Flight System	Six-Instrument Taurus Option	*One-Instrument Taurus Option*
Mission class (A/B/etc.)	B	*B*
Mission lifetime	3.5 years	*3.0 years*
Redundancy	Dual-string	*Dual-string*
Total radiation dose	30 krad	*30 krad*
Peak power mode	Thruster control	*Thruster control*
Peak power (w/contingency)	595.1 W	*431.6 W*
Payload mass	66.5 kg	*5.0 kg*
Spacecraft dry mass	216.8 kg	*160.1 kg*
System dry mass (w/contingency)	368.3 kg	*214.6 kg*
Propellant mass	37.6 kg	*30.9 kg*
Total launch mass	439.5 kg	*245.5 kg*
Reserves	30%	*30%*

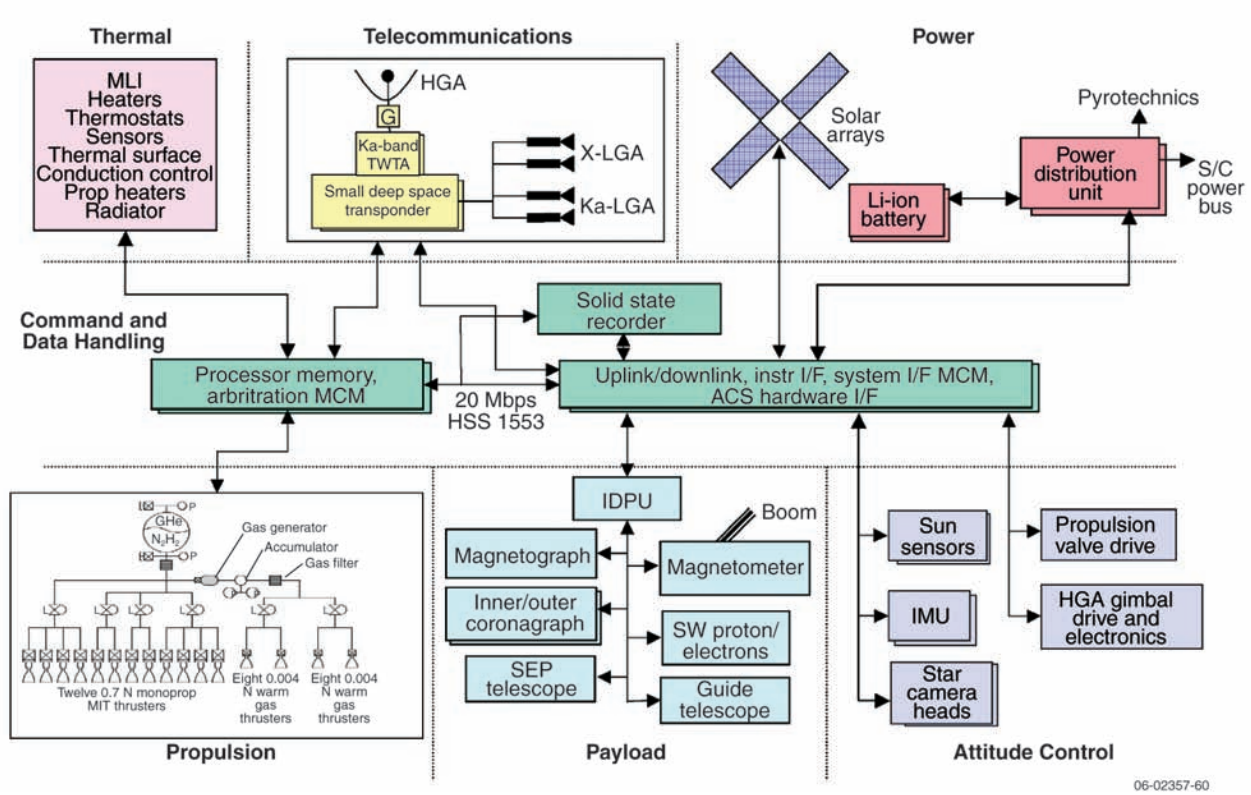

Figure D-7. Flight system block diagram for the Six-Instrument Option.

components are all high-heritage, flight-validated components that are either currently available or will be available by 2012 (4 years prior to the earliest launch date). Aside from the high gain antenna, dual-string redundancy is found throughout the system, including multiple low gain antenna horns, two batteries, two solid-state recorders, two flight computers, and redundant propulsion and ACS subsystems.

Mass and power budget. The mass budget is summarized is in **Table D-9**. These numbers are based on a detailed mass equipment list, which includes current best estimates for each component. These individual estimates are summarized in the table and include cabling and a spacecraft adapter. Additionally, the Taurus 3113 does not include a spacecraft adapter on the launch vehicle side. Therefore, it is included here as 33.6 kg (or 5% of the dry mass). The total launch mass, including 30% contingency for growth, is 439.5 kg.

The power budget is also summarized in **Table D-9**. These numbers are based on a detailed power mode sheet that considers when specific spacecraft components are operated and their respective power levels. The five power modes shown in the table were considered, along with modes for safing and science/telecom. From this analysis, the thruster control power mode is the highest power mode, as shown in the table. During this power mode, most subsystems are operational (including propulsion and telecom), while the instruments are powered off. Adding 30% contingency, the total power required is 595.1 W.

Mechanical design. The FSS mechanical design is a typical cubic spacecraft layout as described in **Table D-10**. Its dimensions allow it to tightly fit within the 1.4-m fairing of a Taurus launch vehicle. There are seven mechanisms, which are primarily used for deploying the four solar arrays, the high gain antenna, and the boom for the magnetom-

Table D-9. Mass and power budget.

Flight System Element	Power (W)
Payload	N/A
C&DH	6.5
Telecom	198.0
Attitude control	72.0
Power	41.6
Propulsion	52.7
Thermal	87.0
Structure	N/A
Subtotal	457.8
Power contingency	137.3 (30%)
Total	**595.1**

Summary of Power Modes	Power (W)
Science	369.2
Instrument calibration (array sizing)	570.8
Thrusters (highest power)	595.1
Cruise/telecom	492.1
Launch (battery sizing mode)	393.8

Flight System Element	Mass (kg)
Payload	66.5
C&DH	12.6
Telecom	22.0
Attitude control	8.8
Power	41.8
Propulsion	13.1
Thermal	19.3
Structure	99.3
Cabling	24.8
S/C adapter	6.5
Subtotal	283.3
Mass contingency	85.0 (30%)
Spacecraft dry mass	368.3
Propellant	37.6
Launch vehicle adapter	33.6 (5%)
Total launch mass	**439.5**
LV capability	445
LV margin	6 (1%)

Table D-10. Mechanical design overview.

Mechanical Design	Six-Instrument Taurus Option	*One-Instrument Taurus Option*
Spacecraft dimensions	0.97 x 0.97 x 0.97 m	*< 0.97 x 0.97 x 0.97 m*
High gain antenna diameter	1.25 m	*1.25 m*
HGA boom length	1.25 m	*1.25 m*
Magnetometer boom length	5.0 m	*N/A*
Number of mechanisms	Solar array deployment (4) HGA 2-axis articulation (1) HGA deployment (1) Mag. boom deployment (1)	SA deployment (4) HGA 2-axis articulation (1) HGA deployment (1)
Number deployments	Solar array deployment (1) HGA deployment (1) Mag. boom deployment (1)	*Solar array deployment (1)* *HGA deployment (1)*

eter. Only the high gain antenna requires additional articulation, allowing it to point toward Earth as the spacecraft drifts to the far side of the Sun. The solar arrays do not require articulation, since the spacecraft is continuously pointed at the Sun, except during launch, trajectory correction maneuvers (TCMs), and events where battery-backup is provided. The One-Instrument Option is similar, but would have a smaller bus size, and it would not have the boom or deployment associated with the magnetometer.

Figure D-8 illustrates the FSS flight system configuration. The solar array has four symmetric wings to minimize disturbances to the control of the flight system. Similarly, the high gain antenna and magnetometer boom are mounted at opposite ends. Internally, the instruments are mounted on a carbon optical bench, which is attached to the top of the spacecraft. Most instruments face outward, directly into the Sun.

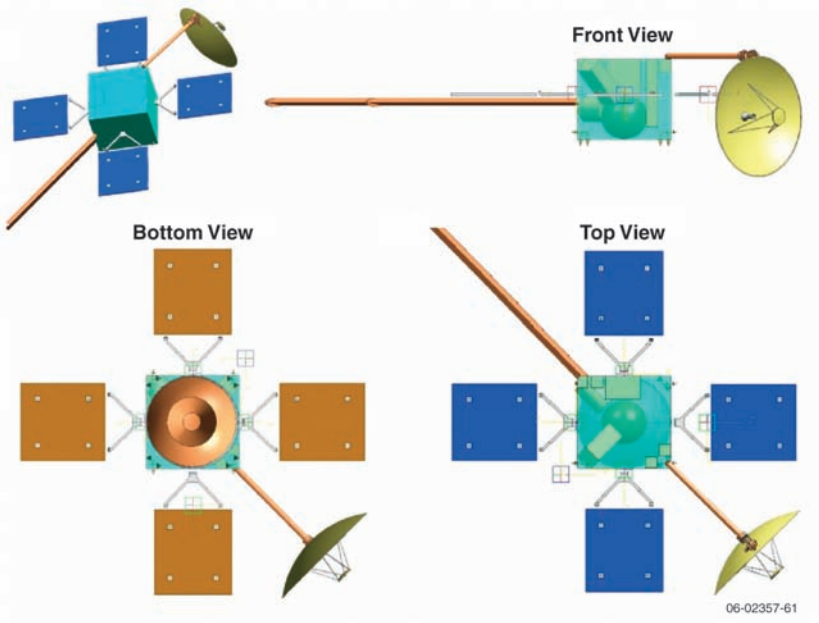

Figure D-8. Flight system configuration.

Thermal control. The thermal control for the spacecraft (**Table D-11**) ensures that all flight subsystems are maintained within their desired thermal ranges. This control accounts for external environmental influences (primarily the Sun between 0.85 and 1.0 AU) and internal power dissipation. Additionally, the science instrument thermal interfaces are monitored to ensure correct thermal control of the integrated instrument module.

To accomplish these objectives, various passive and active elements are used. Passive elements include lightweight multilayer insulation, thermal surfaces, conduction control, and a thermal radiator for the telecom system. Active elements include temperature sensors and electric heaters/thermostats for the propulsion elements, batteries, critical flight elements, and instruments.

Power. The three components of the power subsystem are the solar array, battery, and power electronics. The solar array is used nearly continuously, except during launch and trajectory maneuvers (as necessary). It is sized at 2.24 m^2 to accommodate a peak power of 589.5 W, assuming a maximum heliocentric range of 1.0 AU and the use of state-of-the-art triple-junction technology. Two 50-Ah lithium-ion batteries are used for reserve power and augmentation during high demand modes. These batteries are currently used on short-term missions and will be fully validated for long-term missions by 2012. The power electronics will be packaged in a 6U form factor and support power distribution, battery charge control, bus voltage control, and load-switching function. (See **Table D-12**.) The One-Instrument Option is similar, but relies on smaller 1.27 m^2 solar arrays and 30-Ah batteries to provide for a TCM peak power of 431.6 W.

Telecommunications. The design of the telecom subsystem (**Table D-13**) and DSN coverage are tightly coupled, such that the design can be

Table D-11. Thermal control subsystem parameters.

Thermal Control	Six-Instrument Taurus Option	*One-Instrument Taurus Option*
Number of thermostats	16	*12*
Number of heaters	20	*18*
RF out	27.0 W	*9.0 W*
Radiator size	0.33 m^2	*0.31 m^2*

Table D-12. Power subsystem parameters.

Power	Six-Instrument Taurus Option	*One-Instrument Taurus Option*
Solar array type	GaAs-TJ	*GaAs*
Solar array size	2.24 m^2	*1.27 m^2*
Battery type	Li-Ion	*Li-Ion*
Battery size	50 Ah	*30 Ah*
Power electronics	Power distribution, battery & solar array control, 6U form factor, provide redundancy and single fault tolerance	*Power distribution, battery & solar array control, 6U form factor, provide redundancy and single fault tolerance*

Table D-13. Telecommunications subsystem parameters.

Telecommunications	Six-Instrument Taurus Option	*One-Instrument Taurus Option*
Band (S/X/Ka/etc.)	X-band up Ka-band down	*X-band up* *Ka-band down*
Redundancy	Dual-string	*Dual-string*
High gain antenna size	1.25 m	*1.25 m*
TWTA power	90.0 W	*30.0 W*
Downlink data rate	2.8 Mbps	*0.9 Mbps*
Pointing accuracy	0.1°	*0.1°*
Margin	3.02 dB	*3.42 dB*

optimized for low mass, reduced DSN operations, or a combination thereof. Allowing for a science collection data rate of 115.6 kbps and the Taurus 3113 fairing, the telecom design was optimized to reduce both dry mass and DSN operations. Correspondingly, the minimum DSN coverage is employed, which consists of one 8-hour weekly pass with 36 12-m DSN antennas (using the new DSN array). For this coverage frequency and receiving aperture, a Ka-band downlink rate of 2.8 Mbps is accommodated. The downlink requirement coupled with a 1.25-m high gain antenna on the spacecraft requires a 90.0-W traveling wave tube amplifier (TWTA) to achieve an RF power of 45 W. A pointing accuracy of 0.1° (3σ) is required, which produces approximately 3 dB of margin. Additionally, there are two X-band low gain antenna horns for receiving and two Ka-band low gain antenna horns for transmitting during launch and emergencies. Finally, solar conjunction at the far side of the Sun is a concern, and limited communication should be expected for 20 to 30 days near the conclusion of the primary mission. The One-Instrument Option is similar, but the lower science data collection rate (37.3 kbps) requires only a 30-W TWTA.

Command and data handling (C&DH). The C&DH subsystem is identical for each of the FSS mission concepts considered. Given a technology cutoff date of 2012, the minimum set of avionics hardware identified provides sufficient data processing and storage for all of the options (see **Table D-14**). It is assumed that the multi-chip modules (MCMs) can be micro-packaged on two 6U cPCI cards, all science and ACS instruments will have their own microcontroller/FPGA and data buffer, and the next generation of MSAP (multiservice access platform) electronics will be available. Given these assumptions, the hardware listed in **Table D-14** is a reasonable extension of current technology. This subsystem is dual-string, requiring that each processor be mounted on a separate card and cross-strapped to the two solid-state recorders. This set of advanced electronics will have up to 256 analog channels with an expected design life of at least 8 years.[2]

Software. This mission is similar to a typical deep space mission with payloads nearly identical to STEREO and TRACE, resulting in some code reusability (20–30%) depending on the mission type (see **Table D-15**). The flight software (FSW) must be NASA and CMMI compliant with typical data management and commands for each subsystem. The ACS is the only exception; it requires additional complexity in providing very precise 3-axis stability using the guide telescope. The ACS and guide telescope are tightly linked to provide 20 arcsec of control and 0.1 arcsec of knowledge. The FSW also provides fault protection that monitors, analyzes, and responds to faults, resource management, and timing.

[2]Project should reference the "Design Principles Matrix ID-62432" regarding pre-Phase A design margins for memory allocation for boot code, flight image, hardware interfaces, power, mass, etc.

Table D-14. Command and data handling subsystem parameters.

Command & Data Handling	Six-Instrument Taurus Option	*One-Instrument Taurus Option*
C&DH redundancy	Dual-string	*Dual-string*
Flight computer	Arbitration MCM, Advanced PowerPC processor, 20 Mbps, 50-krad rad-tolerant, 128 analog channels (2)	Arbitration MCM, Advanced PowerPC processor, 20 Mbps, 50-krad rad-tolerant, 128 analog channels (2)
Cards	6U cPCI (2)	6U cPCI (2)
Solid-state recorder	MTO heritage (2)	MTO heritage (2)
Processor speed	240 MIPS	*240 MIPS*
Mass memory requirement	20.0 Gbits/day	*10.0 Gbits/day*
Onboard memory storage	360.0 Gbits	*360.0* Gbits

Table D-15. Software parameters.

Software	Six-Instrument Taurus Option	*One-Instrument Taurus Option*
Autonomy?	No	*No*
Code reusability	20%	*30%*
Subsystem complexity	High ACS complexity	*Med ACS complexity*

Attitude control system (ACS). Given the tight pointing requirements (see **Table D-16**) and the coupling between the ACS and the instrument payload, the complexity and operation of the ACS is fairly high. Originally, reaction wheels were required to meet these requirements. However, a commercially available warm-gas thruster system may be used in conjunction with the hydrazine propulsion system, which significantly reduces complexity.

To accommodate the desired pointing requirements, various assumptions were necessary. The instruments should be integrated and tested as a separate module prior to being assembled to the spacecraft (similar to STEREO). Once the instruments are aligned on a common optical bench, the guide telescope becomes the key boresight reference for all science pointing control and knowledge functions. Thus, the spacecraft can be stabilized on the Sun-line (including pitch, yaw, and roll) using the warm-gas thrusters. Beyond this initial stabilization, the thrusters can use the guide telescope to satisfy the high pointing requirements for pitch and yaw, whereas roll can only be maintained to an accuracy of 20 arcmin (effectively preventing image blurring). This degree of accuracy must be maintained as the spacecraft orbits the Sun at a rate of approximately 1° per day.

It is critical that the instruments are aligned to within 30 arcsec on the integrated instrument module. Following launch, careful instrument calibration during cruise can eliminate this systematic bias. The guide telescope can provide sufficient pointing knowledge to calibrate the payload during cruise. It operates at 50 to 100 Hz with 0.1-arcsec-noise (1σ), which is filtered by the ACS to less than 0.1 arcsec (3σ). Additionally, the magnetograph may also be used in a similar fashion, to produce pointing knowledge (possibly degraded).

The warm-gas thrusters can adequately provide sufficient pointing to eliminate the need for reaction wheels. The gaseous hydrazine is metered by the 4.4-mN Moog thrusters at a feed pressure of 5 psia. The 1 bit (torque impulse bit) of coupled thrusters with 5 ms solenoid actuation time and 0.5 m moment

Table D-16. Attitude control subsystem parameters.

Attitude Control System	Six-Instrument Taurus Option	*One-Instrument Taurus Option*
Stabilization	3-axis	*3-axis*
Pointing control	20 arcsec	*0.1°*
Pointing knowledge	0.1 arcsec (using payload)	*0.1° (instrument provides fine knowledge & stability)*
Pointing stability	<5 arcsec/s	*<5 arcsec/s*
Hardware	Coarse Sun sensors (2) Star trackers (2) Internally redundant IMU Warm gas thrusters (16)	Coarse Sun sensors (2) Star trackers (2) Internally redundant IMU Warm gas thrusters (16)

arms is 22 micro-Nms. Assuming a reasonable spacecraft inertia of 125 Nm^2, the minimum inertia rate is 0.15×10^{-6} rad/s, which is within the required 0.20×10^{-6} rad/s rate derived as the heliocentric angular rate of the instruments. The result is that the thruster one bit quantization satisfies the 20 arcsec control and 5 arcsec/s stability required by the inner and outer coronagraphs.[3]

Propulsion. Since this mission concept does not require large ΔV maneuvers to slow or stop the spacecraft, only a small propulsion system is required. This propulsion system should be sufficient to correct launch injection errors and provide slight adjustments for the lunar gravity assists. The necessary ΔV is estimated at 85 m/s and an additional 20 kg of hydrazine is required for ACS (see **Table D-17**).

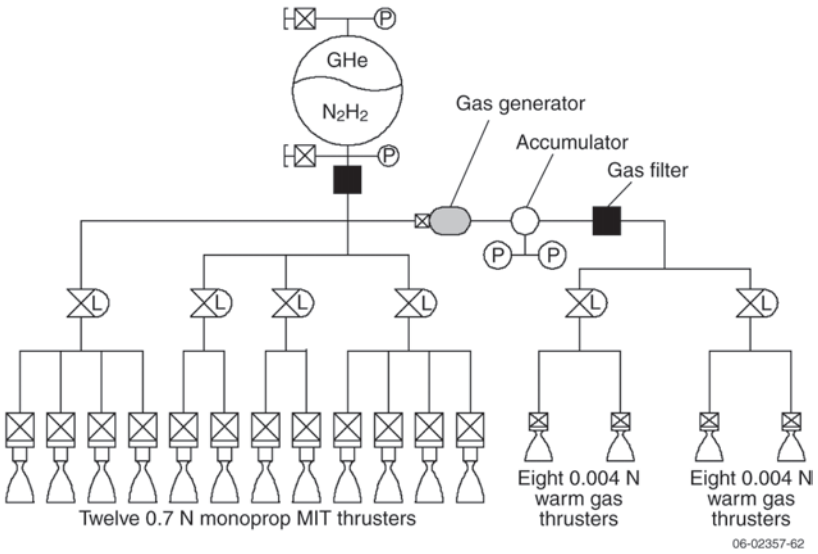

Figure D-9. Propulsion subsystem block diagram.

A block diagram of the propulsion system is shown in **Figure D-9**. A single hydrazine tank holds approximately 30 kg of propellant and pressurant. This fuel feeds to two separate thruster systems. The first thruster system contains two branches of four 0.7-N MIT thrusters that provide thrust for the ΔV burns and pitch/yaw attitude control and two branches of two 0.7 N MIT thrusters for maneuver roll attitude control for a total of 12 thrusters. The second thruster system includes two branches of eight warm gas 0.004-N thrusters for science orbit attitude control. These thrusters are fed by pressure from a warm gas accumulator tank that is maintained by passing hydrazine the through a gas generator based on pressure measurements on the downstream accumulator. The specific thrusters used for this warm gas system are the Moog cold gas thrusters.

[3]A Pointing Control Law will regulate the line-of-sight (LOS) angular rate and position relative to the solar centroid using the IMU and Star Cameras and Guide telescope inputs to a state estimation filter for full state feedback to the rate and position compensator loops that modulate the micro-thruster firings. A feed-forward angular rate signal also may be used based on the heliocentric orbital ephemerides determined by ground tracking and uploaded to the spacecraft.

D.2.4 Ground systems. As previously described, the ground system design and the telecom subsystem are tightly coupled with a necessary trade between increasing mass and power of the telecom transmitter versus adding DSN time and antennas. For the baseline mission concept, a science data collection rate of 115.6 kbps allows for both a relatively small telecom design and a maximum of a single 8-hour weekly DSN pass of 36 12-m antennas during science operations (**Table D-18**).

Cruise tracking and operations occur for the 18 months prior to the start of science operations. During this period, one 4-hour weekly DSN pass with a single 12-m antenna supports navigation tracking, routine spacecraft commanding, health-and-status assessment, and instrument calibration. Additionally, throughout the first 8 weeks after launch, greater 12-m array tracking may be

Table D-17. Propulsion subsystem parameters.

Propulsion	Six-Instrument Taurus Option	*One-Instrument Taurus Option*
Propulsion system	Monopropellant	*Monopropellant*
ACS propellant	20 kg	*20 kg*
Number of 0.7-N thrusters	12	*12*
Number of warm gas thrusters	16	*16*
Isp	225 s	*225 s*

Table D-18. Ground systems overview.

Ground Systems	Six-Instrument Taurus Option	*One-Instrument Taurus Option*
Engineering data rate (uplink)	0.5 kbps	*0.5 kbps*
Engineering data rate (downlink)	2.0 kbps	*2.0 kbps*
Data return overhead	15%	*15%*
Phase E: Cruise		
Link duration	4 hours	*4 hours*
Passes per week	1	*1*
Number of 12-m antennas	1	*1*
Downlink data rate	0.025 Mbps	*0.025 Mbps*
Phase E: Operations		
Link duration	8 hours	*8 hours*
Passes per week	1	*1*
Max number of 12-m antennas	36 (average of 33)	*36 (average of 33)*
Downlink data rate	2.8 Mbps	*0.9 Mbps*

necessary to support the correction of launch vehicle errors, lunar gravity assists, orbit determination, and flight system characterization. For most of cruise, a minimum spacecraft team is required to support instrument operations, gradually increasing as the instrument suite is calibrated prior to the start of science operations. Although a single DSN 12-m antenna should support this level of activity, it is possible that the DSN will only assign the antennas in larger blocks. If so, then the larger block would be used with bi-weekly 4-hour passes, which is the minimum time required for a navigation orbital dynamics solution.

Primary science operations will last for 2 years with tracking provided by the DSN 12-m array. One 8-hour weekly pass is required to support playback of science data, navigation tracking, routine spacecraft commanding, and health-and-status assessment. At the start of the prime mission, the number of required array nodes would increase to 29 12-m antennas, slowly increasing to a maximum of 36 antennas as the distance from Earth to the spacecraft increases. If the mission is further extended, the number of antennas will begin to drop as the spacecraft flies past the far side of the Sun and the range begins to decrease.

Figure D-10 presents a block diagram for the ground system design. There are three major elements, including the spacecraft, the mission operations control center, and the data processing and distribution center. These elements cleanly interact to deliver solar data from the instruments to the science team via the science data archiving system. Along with the delivery of this data, the health of the spacecraft must be continually assessed and commanded as necessary, as illustrated in the figure.

D.3 Schedule

The schedule for design, development, and operations is outlined in **Table D-19**. This schedule follows general Jet Propulsion Laboratory (JPL) design principles, slightly extended given the complexity of developing the integrated instrument module that is mounted on the spacecraft. (The One-Instrument Taurus option shows the recommended baseline mission schedule.) Although the schedule has not been further divided into milestones, testbed development, and hardware deliveries, it is sufficient at this resolution to provide insight into the development, providing additional margin to ensure adequate time for the critical path. Some compression would be possible in a more detailed schedule.

D.4 Summary

There are several potential concepts for the FSS mission, defined primarily by the trajectory and instrument payload options. The trajectories determine the length of overlap with the IHS mission (1.2 to 2.2 years), the minimum solar range (0.8 to 0.85 AU), and the ultimate destination (fixed at 120° or drifting from 60° to 180°). All of these options require interplanetary trajectories and long mission durations that drive the ultimate cost of the mission. The instrument suite is the second principal driver, contributing nearly as much to the development effort as the flight system. Four payload options were considered that range from a simple magnetograph to an instrument suite of the magnetograph,

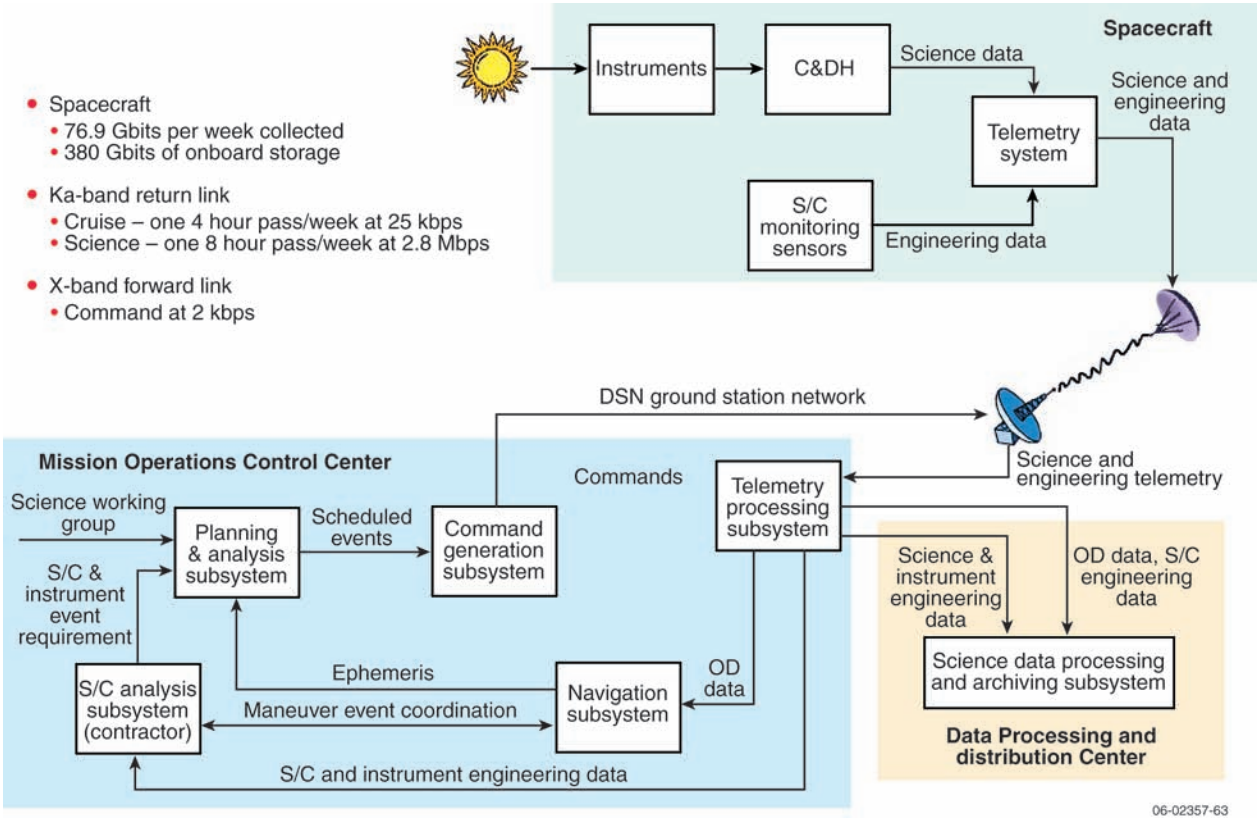

Figure D-10. Ground systems block diagram.

Table D-19. Schedule overview.

Schedule	Six-Instrument Taurus Option	*One-Instrument Taurus Option*
Phase A	7 months	*7 months*
Phase B	12 months	*11 months*
Phase C/D	41 months	*36 months*
Phase E: cruise	18 months	*11 months*
Phase E: operations	24 months	*24 months*
Phase E: data analysis	12 months	*12 months*

coronagraphs, and a package of in situ instruments. Independently from these payload options, data rate was considered as a secondary design driver. Data rates ranging from 37 to 500 kbps can be accommodated across all of the mission concepts, despite slight increases in mass and power.

In parallel, three concepts were studied to support the mission trade space. These options included two complete instrument payloads, differentiated by their trajectories and launch vehicles (Delta II versus Taurus). The third concept emphasized a minimum cost option of a single instrument payload (using a suboptimal trajectory and Taurus launch vehicle). Of these point designs, the Six-Instrument Taurus Option was presented in this report. It is a 3-axis stabilized, redundant flight system. A small propulsion system is required for 85 m/s of ΔV. The telecom system includes a 1.25-m high gain antenna for an X-band uplink and Ka-band downlink that communicates at a rate of 2.8 Mbps (given a continuous science collection data rate of 115.6 kbps). The attitude control system is tightly coupled with guide telescope instrument to provide the precise pointing required by the payload. The pointing control and stability is achieved through a warm-gas thruster system that is equivalent to but less complex than reaction wheels. As a comparison to this option, the key parameters for the One-Instrument Taurus Option were also presented, and additional information is available upon request.

Acknowledgements. Many team members greatly contributed to this effort, including the design and analysis of the payload options, trajectories, mission trade space, and validated point designs. The team members include Jim Chase (study lead), Janine Daughters and Luke Dubord (systems), Chen-wan Yen (mission design), Xiaoyan Zhou, Neil Murphy, Joe Davila, and Adam Szabo (payload), Jerry Flores (configuration), Bob Gustavson (ground systems), Mike Fong (cost), Juan Ayon (oversight), Ed Mettler (ACS), Vince Randolph (C&DH), Sal Distefano (power), Dick Cowley (propulsion), Yu-wen Tung (software), Gerhard Klose (structure), Dave Hansen (telecom), and Bob Miyake (thermal).

This research was funded by the NASA Living with a Star Program Office. It was carried out at the Jet Propulsion Laboratory, California Institute of Technology, under a contract with the National Aeronautics and Space Administration. Reference herein to any specific commercial product, process, or service by trade name, trademark, manufacturer, or otherwise, does not constitute or imply its endorsement by the United States Government or the Jet Propulsion Laboratory, California Institute of Technology.

Appendix E: Engineering Implementation of the Near-Earth Sentinel Payload

The role of the Near-Earth Sentinel (NES) is (1) to characterize the coronal source regions of solar energetic particles (SEPs) and coronal mass ejections (CMEs) and (2) to relate in-situ measurements by the Inner Heliospheric Sentinels (IHS) to the large-scale density structures in the inner heliosphere. NES measurements, when combined with the in-situ measurements by the IHS near 0.25 AU, will provide the information needed to guide the development of new, physics-based models of SEP acceleration and CME initiation. By tailoring the theoretical models to specific events and structures that are observed with remote-sensing and in-situ instrumentation, significant progress can be made in the development of a predictive capability for SEPs. Fully developed models would then be able to use the NES measurements close to the Sun to predict SEP, CME, and solar wind properties measured at the IHS spacecraft and beyond.

NES ultraviolet measurements of spectral line intensities and profiles will be used to determine thermal and non-Maxwellian velocity distributions, densities, and bulk flow velocities for ions and electrons in the extended corona (out to ~10 R_S). Polarized white-light brightness measurements will be used to determine electron densities and velocities of structures in the inner heliosphere (out to 60 R_S). The latter observations will include the inner portions of the IHS orbits and thereby provide a global context for the in-situ measurements of transients as they evolve during their passage through the inner heliosphere.

Combined UV spectroscopy and white-light polarimetry will provide information on SEP source regions, e.g., CME shocks and flare/CME current sheets. In the case of CME shocks, NES observations will be used to determine shock structure, speed, compression ratio, and angle. For flare/CME current sheets, NES observations will be used to determine the current sheet thickness, plasma density, temperature, ion distribution functions, plasma composition, and ion charge states and to estimate magnetic and electric field strengths, helicity, and reconnection rates.

E.1 Mission Summary

Ideally the remote-sensing NES spacecraft should fly in concert with IHS. The start of the primary science phase for NES should overlap as much as possible with the IHS primary mission. The optimal combined observational time period is near solar maximum when the rate of flare/CME events is at its maximum value. The baseline mission will use a launch vehicle capable of placing NES into a 650-km-altitude, Sun-synchronous orbit that provides a nearly continuous observation period without Earth eclipses while avoiding the additional cost associated with a geostationary or L1 mission. The NES spacecraft should be designed for a mission life comparable to that of the primary IHS mission (3 years).

The NES design is very similar to recent solar remote-sensing missions. Hence specific spacecraft bus (SCB) options were not studied in detail. The focus was placed on instrument feasibility studies aimed at extending UV spectroscopic coronagraph and white-light coronagraph capabilities. A Smithsonian Astrophysical Observatory (SAO) team studied improvements to a UV spectroscopic coronagraph, while a Naval Research Laboratory (NRL) team investigated white-light coronagraph implementations. The results of these engineering studies are summarized below.

E.2 Near-Earth Sentinel Baseline Payload

The NES baseline payload consists of a UV Spectroscopic Coronagraph (UVSC), a Wide- and Inner-Field Coronagraph (WIFCO), a Guide Telescope (GT), a Deployable Boom Assembly (DBA), and Instrument Remote Electronics (IRE). The instrument complement can work as individual instruments or as a suite of instruments controlled by a common data processing/instrument controller in the IRE. Details of the NES instrument complement are given in **Table E-1**.

E.2.1 Ultraviolet Spectroscopic Coronagraph (UVSC). The requirement on UVSC is to describe and characterize CMEs, including CME shocks and current sheets, which are believed to be the source regions of solar energetic particles. The instrument is required to have a high enough cadence to describe the evolution of fast CME events. For detailed studies of CMEs, flare/CME current sheets, corona streamers and polar plumes, its spa-

tial resolution should be at least 5 arcsec. Also, UVSC should have a high enough spectral resolution to determine proton and minor ion velocity distributions (thermal and non-Maxwellian). Doppler shifts would also be used to determine bulk velocities along the line of sight. Determination of elemental abundances and charge states of ions in coronal plasmas would be used to identify the origin of particles detected in situ with the IHS spacecraft. In addition, UVSC should be capable of measuring coronal electron temperatures, including departures from a Maxwellian velocity distribution. When combined with white-light density measurements, UVSC observations would be used to determine bulk outflow velocities with the Doppler dimming/pumping technique.

The SAO team determined that a large-aperture, high-sensitivity coronagraph with a filed of view (FOV) that extends from 1.2 to 10 R_s and has an external linear occulter at the end of a 13-m boom can provide the required resolution and cadence. This instrument will have up to 2 orders of magnitude higher sensitivity and a wider spectral range than UVCS on SOHO. This improved performance will allow the determination of line profiles for atoms and ions of many different charge-to-mass ratios, including helium, the most dominant species after hydrogen. The instrument's large aperture and superior stray light suppression permit observations of coronal structure and SEP source regions as close as 1.2 R_S from Sun-center, which is significantly closer to the disk than earlier space-based coronagraphs have been able to achieve. This is particularly important for characterizing CMEs and their associated current sheets right after their formation close to the coronal base. A possible design for UVSC is shown on **Figure E-1**. The overall mass of the instrument, including electronics, is estimated as 265 kg (with 20% margin and 20% reserve). The instrument requires about 135 W average operational power. The technical characteristics for UVSC are provided in column 2, **Table E-1**.

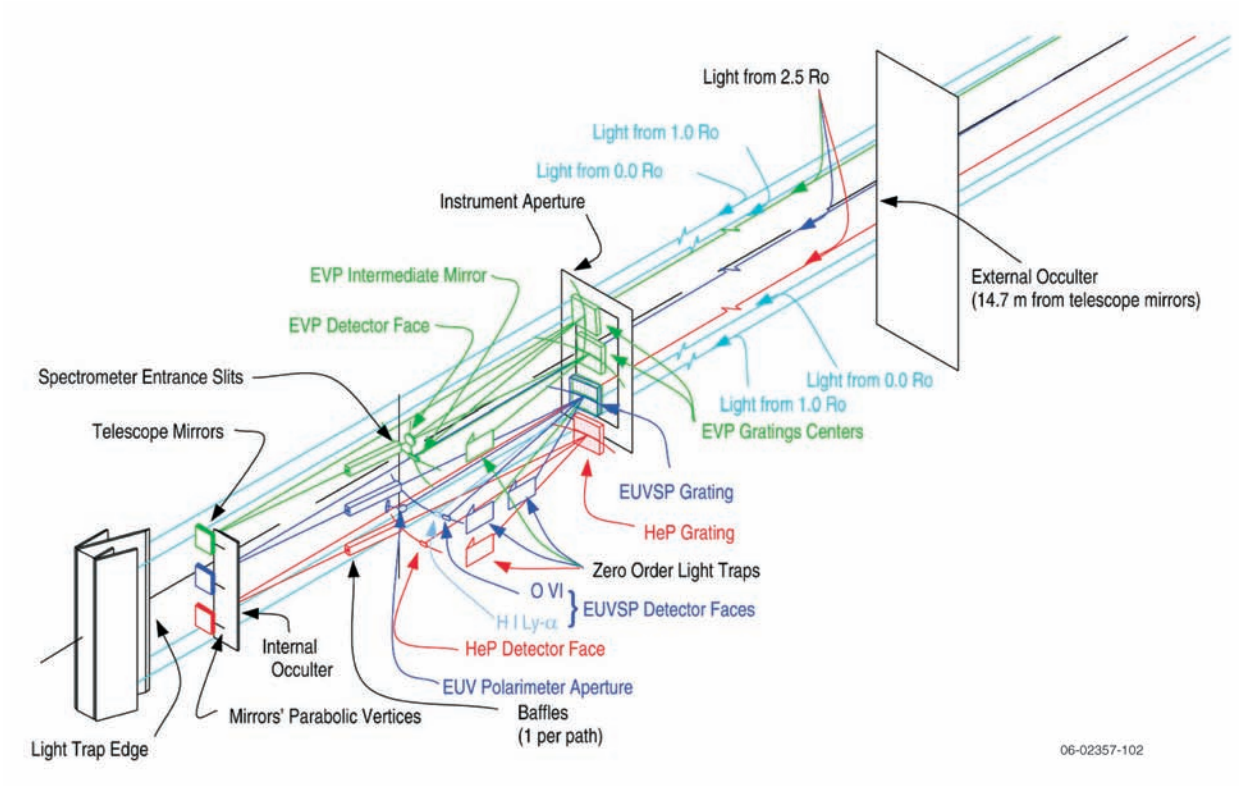

Figure E-1. Ultraviolet Spectroscopic Coronagraph Concept. UVSC has three optical paths, each with an internally occulted telescope mirror, spectrometer entrance slit, grating(s), and a detector. The paths are optimized for measurements of (1) He II 30.4 nm, (2) H I Lyα/OVI 103 nm, and (3) electron scattered H I Lyα. Note that the distance to the external occulter is not shown to scale.

Table E-1. NES instrument characteristics and technical requirements

Parameter/Characteristics	UVSC (Instrument 1)	VLC (Instrument 2)	IFC (Instrument 3)	WFC (Instrument 4)	3 IREs	Comments
Allowable Physical Interfaces						
Unit (launch) volume	230 × 90 × 70 mm	220 × 40 × 110 mm	800 × 470 × 295 mm	800 × 470 × 295 mm	0.35 × 0.35 × 0.35 m enclosure w/cabling (each IRE)	Physical envelopes are based on preliminary launch fairing analyses and are applicable to instrument launch configurations. X axis is the Sun-pointing axis. Electronics volume shown is for a single instrument.
Alignment requirements	Instruments 1, 2 and 3 must have definitive aperture planes and be capable of being coaligned w.r.t. other instrument units, the GT, and the deployable boom (if applicable).				N/A	
Sensor unit (operational)	All instrument deployable cover hardware must reside behind Instrument aperture plane when fully-deployed.				N/A	
Instrument Mech. Interfaces						
Interface mount	Flat-panel hard mount	Flat-panel hard mount	Flat-panel hard mount	Flat-panel hard mount	N/A	Instrument interface, deployable boom, and guide telescope mounts shown are for single instrument mounting.
Boresight w.r.t. SCB roll axis	0°	0°	0°	0°	N/A	
Clear field of view (FOV)	2.5 R_S(Y) × (1.1–10) R_S(Z)	2.5 R_S(Y) × (1.1–10) R_S(Z); (1.1–5.0) R_S (outside UVSC FOV)	1.3-4 R_S	5-60 R_S	N/A	
Deployable boom	4-point hard mount	4-point hard mount	None	None	None	
Guide telescope	If applicable, two 2-point hard mounts (approx. 0.75 m apart)	If applicable, two 2-point hard mounts (approx. 0.75 m apart)	None	None	None	
Instrument Elec. Interfaces						
Command/housekeeping data	See IRE	See IRE	See IRE	See IRE	MIL-STD-1553 bus for each IRE	Power and data interfaces shown are for single instruments.
Science data	See IRE	See IRE	See IRE	See IRE	16-bit parallel bus for each IRE	
Power	See IRE	See IRE	See IRE	See IRE	Reg & Unreg 28-V DC power busses per IRE	
Allowable Mass						
Sensor unit	265 kg	105 kg	20 kg	12.7 kg	N/A	Best estimate plus 20% margin and 20% reserve.
Electronics unit	N/A	N/A	2 kg	2 kg	25 kg per IRE	
Allowable Power						
Average (operational)	135	45	45	45	20 W per IRE	Best estimate plus 20% margin and 20% reserve. The nonop heater power values do not include reserve and margin.
Nonoperational (survival)	85	27	19	19	10 W per IRE	
Imaging Requirements						
FOV	2.5 R_S × (1.2–10) R_S	2.5 R_S × (1.2–10) R_S; (1.2–5.0) R_S (outside UVSC FOV)	1.3-4 Rs	5-60 Rs	N/A	The UVSC instrument requires spacecraft roll maneuvers around the spacecraft–Sun line for pointing.
Spatial resolution element	5.0 × 5.0 arcsec	5.0 × 5.0 arcsec	3.75 arcsec	28 arcsec	N/A	
Pointing Performance						
Absolute pointing (pitch/yaw)	1 arcmin	1 arcmin	50 arcsec	50 arcsec	N/A	
Knowledge (pitch/yaw)	30 arcsec	30 arcsec	30 arcsec	30 arcsec	N/A	
Stability (pitch/yaw over 50 min.)	1.5 arcsec	1.5 arcsec	4 arcsec	4 arcsec	N/A	
Drift (pitch/yaw over 24 h)	10 arcsec	10 arcsec	N/A	N/A	N/A	
Absolute pointing (roll)	40 arcmin	40 arcmin	40 arcmin	40 arcmin	N/A	
Knowledge (roll)	20 arcmin	20 arcmin	20 arcmin	20 arcmin	N/A	
Stability (roll over 50 min)	2 arcmin	2 arcmin	N/A	N/A	N/A	
Drift (roll over 24 h)	12 arcmin	12 arcmin	N/A	N/A	N/A	
Occulting Performance						
Absolute occulting (pitch/yaw)	20 arcsec	20 arcsec	50 arcsec	50 arcsec	N/A	The occulting performance numbers shown here are the total requirements which are allocated among the instruments, the deployable boom, and the SCB. The SCB provides roll and offset pointing maneuvers and achieves stability 30 s after maneuver is completed. Absolute roll pointing is determined by spacecraft roll pointing.
Knowledge (pitch/yaw)	10 arcsec	10 arcsec	30 arcsec	30 arcsec	N/A	
Stability (pitch/yaw over 24 h)	5 arcsec	5 arcsec	4 arcsec	4 arcsec	N/A	
Absolute occulting (roll)	N/A	N/A	40 arcmin	40 arcmin	N/A	
Knowledge (roll)	N/A	N/A	20 arcmin	20 arcmin	N/A	
Stability (roll over 24 h)	N/A	N/A	N/A	N/A	N/A	
Thermal						
Operating temperature range	10 to 30°C	10 to 30°C	10 to 30°C	10 to 30°C	0 to 40°C	The SCB/Instrument thermal interface assumes a highly isolated design in which radiative and conductive coupling are minimized.
Standby temperature range	10 to 30°C	10 to 30°C	10 to 30°C	10 to 30°C	0 to 40°C	
Survival temperature range	0 to 40°C	0 to 40°C	0 to 40°C	0 to 40°C	–10 to 50°C	
Data Rates						
Housekeeping	3.00×10^3 bps	2.00×10^3 bps	2.00×10^3 bps	2.00×10^3 bps	N/A	
High-speed science data	5.60×10^6 bps	8.00×10^6 bps	1×10^6 bps	1×10^6 bps	N/A	
Average data rate	1.60×10^6 bps	5.40×10^6 bps	2.30×10^5 bps	2.30×10^5 bps	N/A	

UVSC = Ultraviolet Spectroscopic Coronagraph; VLC = Visible Light Coronagraph; IFC = Inner Field Coronagraph; WFC = Wide Field Coronagraph; IRE= Instrument Remote Electronics; SCB = Spacecraft Bus

E.2.2 Wide- and Inner-Field Coronagraph (WIFCO). WIFCO consists of a Wide Field Coronagraph (WFC) and an Inner Field Coronagraph (IFC) combination. As noted below, there is an option to replace the IFC with a more capable large-aperture visible light coronagraph (VLC).

Wide Field Coronagraph (WFC). The Sentinels science objectives require concurrent in-situ and remote observations of the same heliospheric structures. WFC should be able to image shocks and CMEs to heliocentric distances of ~60 R_S (~0.3 AU), which overlaps a portion of the IHS orbits (perihelion of ~0.25 AU). The temporal resolution should be sufficient to track the evolution of shocks and fast CMEs associated with the acceleration of SEPs. The fastest of the 10,000 CMEs recorded by LASCO had a speed of 3200 km/s, on November 10, 2004; the second-fastest traveled at 2800 km/s; and 36 CMEs have had speeds above 2000 km/s. Since the maximum proper motion of a 2000 km/s CME is 1 R_S in 5.8 min, these structures would be well recorded with WFC cadences of 2 min inside 6 R_S, 10 min inside 12 R_S, and 20 min from 12 to 60 R_S.

Image quality can be expressed in terms of exposure, spatial resolution, exposure time, and masking of coronal structure by energetic particles during radiation storms. Exposure sufficient to detect CMEs and shocks in the outer field of view can be estimated by scaling from LASCO/C3, which detects shocks to about 25 R_S. The required exposure, where both signal and background profiles are taken into account, is about 12 times that achieved in 19 s with LASCO/C3. Spatial resolution required to detect CME and shock structures is ideally about 30 arcsec per pixel, where spatial resolution is dominiated by detector pixelation; but it could be as high as about 100 arcsec, since the structures are relatively broad. Exposure time short enough to avoid image smear beyond about 30 arcsec for fast CMEs and shocks is about 10.8 s. Energetic particles incident on the WFC image detector can mask CME and shock data during SEP events. The radiation storm of 22 November 2001, associated with a flare and halo CME, was the sixth-ranked proton storm from 1976 to 2003, and had a peak >10 MeV proton flux equal to 0.44 of the largest storm in the 27-year period. The corresponding peak masked pixel fraction for the LASCO CCD was 0.8 with a 19-s exposure time, 22-s read time, and 21 × 21 µm pixels. Good WFC imagery can be maintained during the worst storms with multiple short 3-s exposures (peak masked fraction ~0.1; 13.5 × 13.5 µm pixel), obtained within the image blur time, that are efficiently scrubbed onboard for energetic particles before summing to a single final image.

A WFC instrument concept (**Figure E-2**) was developed by an NRL team consistent with the above requirements by scaling from the 33 R_S half FOV SOHO/LASCO/C3 to 60 R_S. A larger 21-mm diameter entrance aperture, A1, was chosen to increase light-gathering power by nearly a factor of 6, partially satisfying the exposure requirement, while image summing was introduced to both satisfy the remaining exposure requirement and accomplish the energetic particle scrubbing. A single 3-s exposure will be adequate to 25 R_S Five 3-s exposures summed onboard will be adequate for 60 R_S.

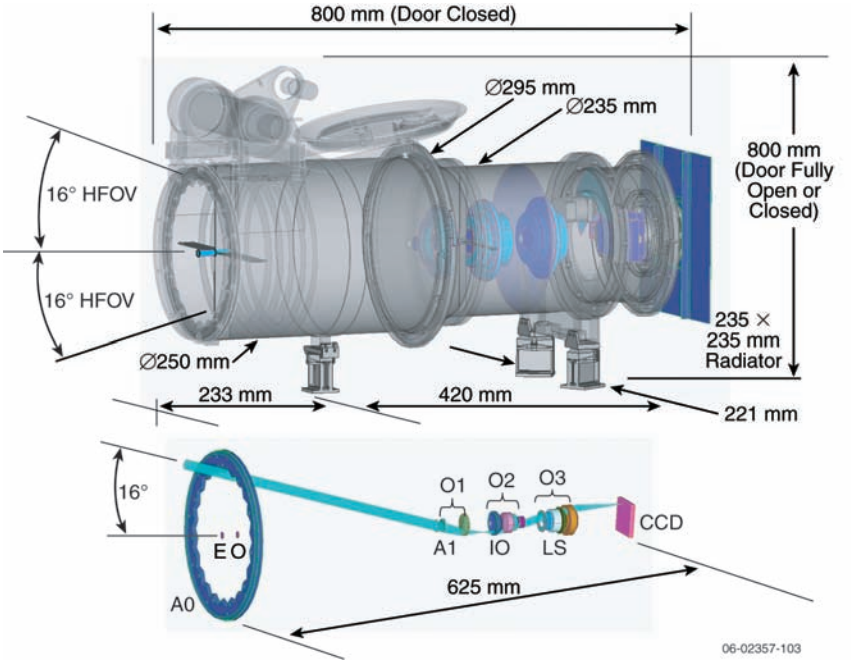

Figure E-2. Wide Field Coronagraph (WFC) concept showing the envelope and optical layout. EO = external occulter; A0 = first aperture; A1 = entrance aperture; LS = Lyot stop; CCD = charge couple device; O1, O2, and O3 = lens subassemblies 1, 2, and 3.

ZEMAX ray trace analysis was performed to define the optical train and its image performance. Instrumental stray light over the field of view would be comparable to LASCO/C3. A polarization analysis capability is recommended to improve knowledge of the three-dimensional distribution of the CMEs and shocks with respect to the IHS.

The CCD image reading, scrubbing, and summing are assumed to take place in a camera electronics box (CEB) located near the detector. All other mechanisms, as well as thermal control, are assumed to be located in a common instrument processing unit. The WFC technical characteristics are provided in column 5, **Table E-1**.

Inner Field Coronagraph (IFC). Rather than requiring WFC to observe coronal structure down to the lower corona, the separate IFC is suggested to cover the range from ~1.3 to 4 R_S The IFC is a high spatial and temporal resolution instrument that records the onset, structure, and initial acceleration of CMEs and possibly shocks in SEP source regions low in the corona and near the solar limb. It has a Sun-centered circular field of view that should, at its inner limit, approach the solar limb to capture events that are out of the plane of the sky. The spatial resolution should be better than 10 arcsec to detect CME substructure. The timing of CME onset should be accurate to about 1 min in order to relate the coronagraphic observations with SEP timing analysis using IHS data. The acceleration and velocity of the fastest CMEs should be observable, since these are associated with shocks and SEP acceleration.

A classical Lyot coronagraph will detect the required CME and shock density signatures in the electron, or K-corona, with a simple and compact instrument operating with a broad passband in the visible region of the spectrum where the K-corona signal peaks. Internal occultation is required to achieve high spatial resolution near the inner field limit (~1.3 R_S). With a compact instrument, this type of occultation limits the outer field cutoff to about 4 R_S due to the scatter of solar disk light by the objective into the coronal image.

The flight-qualified STEREO/SECCHI/COR1[1] is typical of a coronagraph that could be built and operated to satisfy the NES requirements. **Figure E-3** is a conceptual design of this instrument. The coronagraph uses a polarization analyzer to enhance the contrast of the polarized K-corona Thomson scattered photospheric photon signal in the presence of the unpolarized scene F-corona and instrumental backgrounds. The exposure time is short enough that fast CME image smear and energetic particle masking of the image at the CCD are minimal. We use a nominal value of 2000 km/s for a "fast" CME. CMEs with velocity above 2000 km/s are observable with some small image degradation. Approximately eight images of a fast CME can be used to determine velocity and acceleration before it passes beyond the outer 4-R_S FOV cutoff. The instrument technical characteristics for IFC, as determined by the NRL team, are provided in column 4, **Table E-1**.

[1]Thompson, W. T., et al, COR1 inner coronagraph for STEREO-SECCHI, in: *Innovative Telescopes and Instrumentation for Solar Astronphysics*, SPIE Proceedings Vol. 4853, eds. S. L. Keil and S. V. Avakyan, p.1, SPIE, Bellingham, WA, 2003.

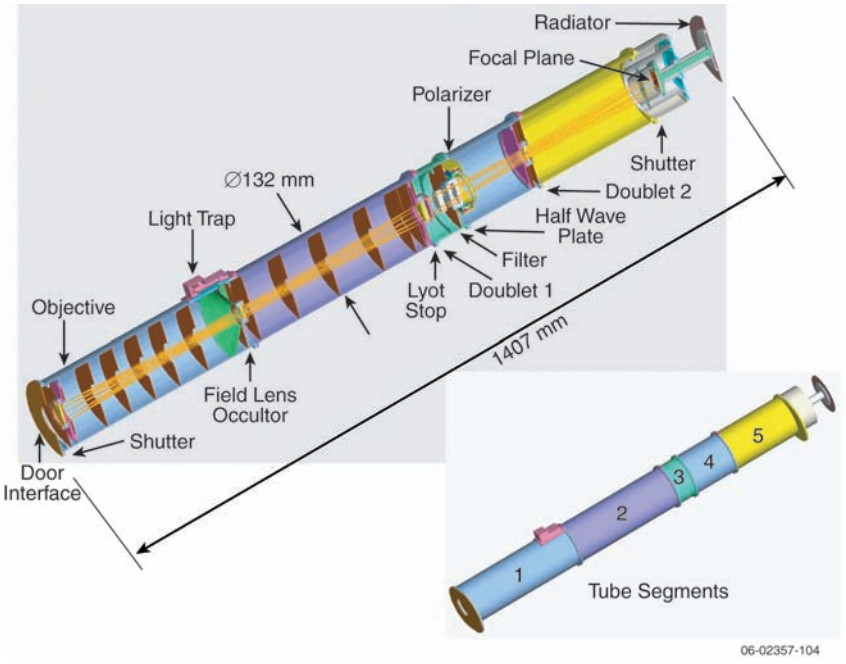

Figure E-3. Inner Field Coronagraph (IFC) concept. The section view of the IFC reveals the standard Lyot design beginning with the 36-mm diameter objective lens, which is followed by the internal occulter, field lens, Lyot stop, bandpass filter, polarization analyzer, transfer lens, shutter, CCD detector and CCD radiator.

Optionally, a more capable large-aperture coronagraph that takes advantage of the UVSC occulting boom could be used instead of the IFC. The Visible Light Coronagraph (VLC), studied by the SAO team, is a large-aperture, broadband visible light coronagraph that will provide a time series of polarized brightness images of the corona from 1.2 to 10 R_S. These data are used to provide high-spatial-resolution (5 arcsec) and high-temporal-resolution (10-s cadence) maps of the electron density distribution in coronal holes, streamers, and CMEs. The externally occulted VLC has superior stray light suppression and a spatial resolution in the radial direction (inside of 2 R_s) that is an order of magnitude better than any previously flown coronagraph. The external occulter supported by a 13-m boom allows the optical system to resolve structures such as the tops of CME flux ropes with "eclipse-like" clarity. The VLC would provide information on the coronal density structure and bulk flows that could be used with spectroscopic data provided by the UVSC to characterize CME, SEP, and solar wind source regions. The high time cadence is required for detailed studies of CME evolution and would be used to investigate the wave propagation of density perturbations in coronal structures. Technical specifications of this instrument are given in column 3 of **Table E-1**.

E.2.3 Guide Telescope (GT). The GT provides error signals to the spacecraft attitude control system (ACS) for maintaining the overall required pointing control. Its design is based on the guide telescope used for the STEREO mission. It provides 5-arcsec absolute accuracy and knowledge and, when combined with the spacecraft attitude control system, provides a 1-arcsec (3σ) pitch/yaw and 5 arcmin (3σ) roll stability. It is to be mounted on one of the instrument structures to ensure precise alignment and control. The required GT characteristics are provided in **Table E-2**.

E.2.4 Deployable Boom Assembly (DBA). The DBA has a 13-m boom with an external occulter system used by the UVSC. At launch the DBA is in a compact retracted configuration but is deployed by the spacecraft bus shortly after launch and remains deployed for the duration of the mission. It carries a linear occulter for UVSC. If a VLC were used in place of the IFC, the boom would also carry a circular occulter. These remote external occulters create an artificial eclipse with an umbra large enough to accommodate the telescope primary mirror while subtending a small enough solid angle to allow observations at 1.2 R_S from the Sun center. The small angular spread of diffracted light from the external occulter also results in exceptional stray light suppression. The WFC and IFC will be co-aligned to the UVSC but do not require the boom. The physical properties, dynamic characteristics, and positional stability requirements are listed in **Table E-3**.

Table E-2. Guide Telescope (GT)—fine-pointing sensor.

GT Parameter/Characteristics	Value	SCB Provisions/Comments
Physical/Resource Properties		
Volume	2.00 × 0.3 × 0.3 m	Mass does not include thermal control materials or associated cabling (SCB provided).
Field of view	2° × 2°	
Mass	3.5 kg	
Power	5 W	
Sensing Performance		
Absolute accuracy	5 arcsec	The GT sensing performance shown here has to be combined with the SCB pointing performance to determine the overall absolute pointing performance.
Knowledge	5 arcsec	
Bias magnitude	30 ± 3 arcsec	
Bias drift	±1 arcsec/month	

Note: SCB = Spacecraft Bus.

Table E-3. Deployable boom assembly (DBA) (SCB = Spacecraft Bus).

DBA Parameter/Characteristics	Value	SCB Provisions/Comments
Physical/Resource Properties		
Volume (stowed)	1.3 × 0.5 × 0.5 m	Cannister has circular cross-section of about 0.5 m diameter.
Mast cross-section	12 × 12 in. (17-in. diagonal)	
Mass	37 kg	
Length	13 m	
Tip mass (maximum at mast end)	5 kg	
Power (deployment)	30 W continuous, 60 W peak	
Dynamic Characteristics		
Deployment rate	< 0.5 in./s	
Structural frequency (stowed)	> 35 Hz	
Structural frequency (deployed)	1.1 Hz	
Design life	280 cycles	
Tip Positional Stability		
Pitch/yaw (long-term)	2 arcmin	
Roll (long-term)	4 arcmin	
Pitch/Yaw (50 min)	20 arcsec	
Roll (50min)	3 arcmin	

Note: SCB = Spacecraft Bus.

APPENDIX F: ACRONYMS AND ABBREVIATIONS

ACE	Advanced Composition Explorer
ACS	Attitude Control System
AIA	Atmosphere Imaging Assembly on SDO
APL	The Johns Hopkins University Applied Physics Laboratory
ATST	Advanced Technology Solar Telescope
AU	Astronomical Unit
BAPTA	Bearing and Power Transfer Assembly
bps	Bits per Second
BWG	Beam Waveguide
C&DH	Command and Data Handling
C_3	Maximum Required Launch Energy
CCD	Charge-Coupled Device
CCSDS	Consultative Committee for Space Data Systems
CPU	Central Processing Unit
CFDP	CCSDS File Delivery Protocol
CIR	Co-rotating Interaction Region
CISM	Center for Integrated Space Weather Modeling
CM	Center of Mass
CME	Coronal Mass Ejection
CMMI	Capability Maturity Model Integration
CP	Center of Pressure
CZT	Cadmium-Zinc-Telluride
DC	Direct Current
DDOR	Delta-Differential One-way Ranging
DOD	Depth of Discharge
DPM	Despun Platform Multiplexer
DPU	Data Processing Unit
DSAD	Digital Solar Aspect Detector
DSN	Deep Space Network
EIT	Extreme Ultraviolet Imaging Telescope on SOHO
ELV	Expendable Launch Vehicle
EMC	Electromagnetic Cleanliness
EPI	Energetic Electron and Proton Instrument
ESA	European Space Agency
EUV	Extreme Ultraviolet
FASR	Frequency-Agile Solar Radiotelescope
FAST	Fast Auroral Snapshot Explorer
FIP	First Ionization Potential
FOV	Field of View
FPGA	Field-Programmable Gate Array
FPI	Fabry-Perot Interferometer
FSM	Farside Sentinel Magnetograph
FSS	Farside Sentinel
FSW	Flight Software
FUV	Far Ultraviolet
G&C	Guidance and Control
GLE	Ground Level Event
GOES	Geostationary Operational Environmental Satellite
GRS	Gamma-Ray Spectrometer
GSFC	NASA Goddard Space Flight Center
HICA	High-Energy Ion Composition Analyzer
HGA	High-Gain Antenna
HPF	High Pass Filter
ICME	Interplanetary Coronal Mass Ejection
IDPU	Instrument Data Processing Unit
IEM	Integrated Electronics Module
IFC	Inner-Field Coronagraph
IHS	Inner Heliospheric Sentinel
IMF	Interplanetary Magnetic Field
IMP	Interplanetary Monitoring Platform
IMU	Inertial Measurement Unit
ISEE	International Sun-Earth Explorer
IST	Interdisciplinary Science Team
JHU/APL	The Johns Hopkins University Applied Physics Laboratory
JPL	Jet Propulsion Laboratory
kbps	Kilobits per Second
KSC	Kennedy Space Center
LASCO	Large Angle and Spectrometric Coronagraph on SOHO
LGA	Low-Gain Antenna
LICA	Low-Energy Ion Composition Analyzer
LV	Launch Vehicle
LVPS	Low Voltage Power Supply
LWS	Living With a Star
MAG	Magnetometer
MC	Magnetic Cloud
MCM	Multi-Chip Module

MESSENGER	MErcury Surface, Space ENvironment, GEochemistry, and Ranging
MGA	Medium-Gain Antenna
MHD	Magnetohydrodynamics
MIPS	Millions of Instructions per Second
MLI	Multilayer Insulation
MOF	Magneto-Optical Filter
MOI	Moment of Inertia
MURI	Multidisciplinary University Research Initiative
MWA-LFD	Mileura Widefield Array—Low Frequency Demonstrator
N/A	Not Applicable
NASA	National Aeronautics and Space Administration
NES	Near-Earth Sentinel
NOAA	National Oceanic and Atmospheric Administration
NS	Neutron Spectrometer
OCXO	Oven Controlled Crystal Oscillator
OSO	Orbiting Solar Observatory
OSR	Optical Solar Reflector
PDU	Power Distribution Unit
PI	Principal Investigator
PPT	Peak Power Tracking
PSE	Power System Electronics
Q/A	Charge-to-Mass
QTN	Quasi-Thermal Noise
RF	Radio Frequency
RHESSI	Reuven Ramaty High Energy Solar Spectroscopic Imager
rpm	Revolutions per Minute
R_S	Solar Radius
RX	Receiver
S/C	Spacecraft
S/N	Signal-to-Noise Ratio
SAMPEX	Solar Anomalous and Magnetospheric Particle Explorer
SCB	Spacecraft Bus
SCM	Search Coil Magnetometer
SDO	Solar Dynamics Observatory
SDRAM	Synchronous Dynamic Random Access Memory
SEP	Solar Energetic Particle
SEPQ	Solar Energetic Particle Composition and Charge State Analyzer
SMM	Solar Maximum Mission
SOHO	Solar and Heliospheric Observatory
Solwind	White-Light Coronagraph on Air Force Satellite P78-1 (1979–1985)
SPE	Solar Particle Event
SSD	Silicon Semiconductor Detector
SSR	Solid-State Recorder
STDT	Science and Technology Definition Team
STEREO	Solar-TErrestrial RElations Observatory
STM	Systems Trade Model
SWComp	Solar Wind Composition Analyzer
SWE	Solar Wind Electron Analyzer
SWI	Solar Wind Ion Analyzer
STE	Suprathermal Electron Instrument
TCM	Trajectory Correction Maneuver
TOF	Time of Flight
TRACE	Transition Region and Coronal Explorer
TR&T	Targeted Research and Technology
TSS	Thermal Synthesizer Model
TWTA	Traveling Wave Tube Amplifier
TX	Transmitter
USN	Universal Space Network
UVCS	Ultraviolet Coronagraph Spectrometer on SOHO
UVSC	Ultraviolet Spectroscopic Coronagraph on the Near-Earth Sentinel
VGA	Venus Gravity Assist
VHP	Venus Hyperbolic Excess Velocity
VLC	Visible Light Coronagraph
VSE	Vision for Space Exploration
WAVES	Radio and Plasma Waves Instrument
WFC	Wide-Field Coronagraph
WIFCO	Wide- and Inner-Field Coronagraph
XEPF	Extended Payload Fairing
XMTR	Transmitter
XPDR	Transponder

REPORT DOCUMENTATION PAGE

Form Approved
OMB No. 0704-0188

1. REPORT DATE *(DD-MM-YYYY)*	2. REPORT TYPE	3. DATES COVERED *(From - To)*
31-07-2006	Technical Memorandum	

4. TITLE AND SUBTITLE

Solar Sentinels:
Report of the Science and Technology Definition Team

5a. CONTRACT NUMBER

5b. GRANT NUMBER

5c. PROGRAM ELEMENT NUMBER

6. AUTHOR(S)

The LWS Sentinels Science and Technology Definition Team

5d. PROJECT NUMBER

5e. TASK NUMBER

5f. WORK UNIT NUMBER

7. PERFORMING ORGANIZATION NAME(S) AND ADDRESS(ES)

Goddard Space Flight Center
Greenbelt, MD 20771

8. PERFORMING ORGANIZATION REPORT NUMBER

2006-214137

9. SPONSORING/MONITORING AGENCY NAME(S) AND ADDRESS(ES)

National Aeronautics and Space Administration
Washington, DC 20546-0001

10. SPONSORING/MONITOR'S ACRONYM(S)

11. SPONSORING/MONITORING REPORT NUMBER

TM-2006-214137

12. DISTRIBUTION/AVAILABILITY STATEMENT

Unclassified-Unlimited, Subject Category:
Report available from the NASA Center for Aerospace Information,7121 Standard Drive, Hanover, MD 21076. (301)621-0390

13. SUPPLEMENTARY NOTES

14. ABSTRACT

The goal of NASA's Living With a Star (LWS) program's is to develop the scientific understanding necessary to effectively address those aspects of the connected Sun-Earth system that directly affect life and society. Along with the other elements of LWS, Solar Sentinels aims to discover, understand and model the heliospheric initiation, propagation and solar connection of those energetic phenomena that adversely affect space exploration and life and society here on Earth. The Solar Sentinels mission will address the following questions: (1) How, where, and under what circumstances are solar energetic particles (SEPs) accelerated to high energies and how do they propagate through the heliosphere? And (2) How are solar wind structures associated with these SEPs, like CMEs, shocks, and high-speed streams, initiated, propagate, evolve and interact in the inner heliosphere? The Sentinels STDT recommends implementing this mission in two portions, one optimized for inner heliospheric in-situ measurements and the other for solar remote observations. Sentinels will greatly enhance the overall LWS science return.

15. SUBJECT TERMS

Solar energetic particles, coronal mass ejections, interplanetary shocks, solar flares, heliospheric plasma and magnetic fields

16. SECURITY CLASSIFICATION OF:			17. LIMITATION OF ABSTRACT	18. NUMBER OF PAGES	19b. NAME OF RESPONSIBLE PERSON
a. REPORT	b. ABSTRACT	c. THIS PAGE			Haydee M. Maldonado
Unclassified	Unclassified	Unclassified	Unclassified	176	19b. TELEPHONE NUMBER *(Include area code)* (301) 286-6762